INELASTIC BEHAVIOR OF TWO-SPAN CONTINUOUS BEAMS SUBJECTED TO MOVING LOADS

Thesis for the Degree of M. S.

MICHIGAN STATE UNIVERSITY

Shien Tsun Wang

1964

I

experim
symmetr
unsprun
made of
6 ft. l
section

varied
that wo
was var

relativ
resulti
mid-spa
involve
"jumps"
loses c
"landed

ABSTRACT

INELASTIC BEHAVIOR OF TWO-SPAN CONTINUOUS BEAMS SUBJECTED TO MOVING LOADS

by Shien Tsun Wang

The purpose of the investigation is to study experimentally the elasto-inelastic behavior of two-span symmetrical continuous beams subjected to a single unsprung load or sprung load. All beams tested were made of mild steel (average yield stress 27,500 psi), 6 ft. long (3 ft. each span), and have a rectangular cross-section of 1" x 1/4".

In the test program the weight of the load was varied from 0.56 to 1.8 times the minimum static load that would first cause yielding in the beam; the speed was varied from 0.2 fps to 15.3 fps.

Results show that a heavy load moving at a relatively slow speed can cross the beam smoothly. The resulting permanent displacement is larger at the first mid-span than at the second mid-span. In tests that involved either a heavy load or a high speed, the load "jumps" as it approaches the middle support, i.e., it loses contact with the surface of the beam, and then "landed" back on the beam at a short distance from the

middle

this ca

span.

at the

tests i

set is

middle support. The resulting permanent displacement in this case is larger in the second span than in the first span. The maximum value of the permanent displacement at the first and the second mid-spans observed in all the tests is 0.6426". In most cases, however, the permanent set is less than 0.14".

INELASTIC BEHAVIOR OF TWO-SPAN CONTINUOUS BEAMS SUBJECTED TO MOVING LOADS

By

SHIEN TSUN WANG

A THESIS

Submitted to
Michigan State University
in partial fulfillment of the requirements
for the degree of

MASTER OF SCIENCE

Department of Civil Engineering

1964

investig

to movi

Engineer

been spo

Grant No

Research

experime

R. Hills

used in

Steel Co

of that

bars use

which ha

Wen to w

instruct

also to

their co

ACKNOWLEDGMENTS

The work reported herein was done as part of an investigation of the inelastic behavior of beams subjected to moving loads conducted in the Department of Civil Engineering of Michigan State University. The project has been sponsored by the National Science Foundation under Grant No. G12143 administered by the Division of Engineering Research.

This investigation represents a continuation of the experimental study on simply supported beams made by Mr. R. Hills who had designed most of the experimental set-up used in this study. Thanks are expressed to Bethlehem Steel Company and Dr. I. M. Viest, Structural Engineer of that organization, for arranging to supply the steel bars used in this study.

This report also constitutes the author's thesis which has been written under the direction of Dr. R. K. Wen to whom gratitude is extended for his guidance and instruction. The author wishes to express his appreciation also to the Machine Shop of the College of Engineering for their cooperation.

Chapte

I.

II.

TABLE OF CONTENTS

Chapter		Page
I.	INTRODUCTION	1
	1.1. Object and Scope	1
	1.2. Notation	3
II.	EXPERIMENTAL WORK	4
	2.1. Experiment Set-up	4
	2.1.1. General	4
	2.1.2. Test Beams	4
	2.1.3. Load Carriage	5
	2.1.4. Driving System	6
	2.1.5. Load Arrester	6
	2.1.6. Abutments, Accelerating, Decelerating Tracks, Monorails and Guide Plates	6
	2.2. Measurements and Instrumentation	7
	2.2.1. Beam Deflections	7
	2.2.2. Carriage Reaction	7
	2.2.3. Load Position	8
	2.3. Stress-Strain and Moment-Curvature Relations	8
	2.3.1. Stress-Strain Relation	8
	2.3.2. Moment-Curvature Relation	9
	2.4. Static Behavior of Continuous Beam	10
	2.4.1. Theoretical Analysis	10
	2.4.2. Experiment Behavior	12
	2.5. Test Program	12
	2.5.1. Parameters of Study	12
	2.5.2. Unsprung Load Test	13
	2.5.3. Sprung Load Test	14

Chapter Page

III. RESULTS OF INVESTIGATION 15

3.1. Unsprung Loads 15

3.1.1. Typical Patterns of Behavior 15

3.1.1.1. Behavior with "Medium"Value of α and "Medium" Value of β 15
3.1.1.2. Behavior with "Small" Value of α and "Large" Value of β 16
3.1.1.3. Behavior with "Medium" Value of α and "Large" Value of β 18
3.1.1.4. Behavior with "Large" Value of α and "Medium" Value of β 20

3.1.2. "Jump" Phenomenon 20
3.1.3. Maximum Mid-Span Dynamic Deflections 22
3.1.4. Mid-Span Permanent Deflections 23
3.1.5. Maximum Acceleration of Load 24
3.1.6. Deformation Under Repeated Loading 25
3.1.7. Permanent Curvature and "Hinge Length" 26

3.2. Sprung Loads 29

3.2.1. Typical Patterns of Behavior 29

3.2.1.1. Behavior with "Medium" Value of α and "Medium" Value of β 29
3.2.1.2. Behavior with "Small" Value of α and "Large" Value of β 31
3.2.1.3. Behavior with "Medium" Value of α and "Large" Value of β 31
3.2.1.4. Behavior with "Large" Value of α and "Medium" Value of β 33

3.2.2. "Jump Line" 33
3.2.3. Maximum Mid-Span Dynamic Deflections 33
3.2.4. Maximum Spring Force 34

THE

Chapte

IV.

LIST OF

FIGURES

Chapter Page

IV. SUMMARY AND CONCLUSION 35

4.1. Summary 35
4.2. Discussion and Conclusion 37

LIST OF REFERENCES 39

FIGURES 40

LIST OF FIGURES

Figure		Page
1.	Overall view of test set-up	41
2.	Load carriage	41
3.	Test beam and differential transformers	42
4.	Driving system	42
5.	Load arrestor	43
6.	Typical stress-strain curve	44
7.	Moment-curvature diagram	44
8.	Curves of yield load and collapse load	45
9.	Deflection at point of loading	46
10.	Static behavior of two-span continuous beam	47
11.	Dynamic test record for unsprung case: $\alpha = 0.05623$, $\beta = 1.0$	48
12.	Dynamic test record for unsprung case: $\alpha = 0.04468$, $\beta = 1.6$	49
13.	Distribution of residual moment	50
14.	Final deformed shapes	50
15.	Dynamic test record for unsprung case: $\alpha = 0.06108$, $\beta = 1.6$	51
16.	"Jump lines"	52
17.	Location of starting position of jump	53
18.	Maximum deflection of first mid-span (unsprung case)	54
19.	Maximum deflection of second mid-span (unsprung case)	55
20.	Location of load for maximum deflection of first mid-span (unsprung case)	56

Figure		Page
21.	Location of load for maximum deflection of second mid-span (unsprung case)	57
22.	Permanent deflection of first and second mid-spans	58
23.	Maximum vertical acceleration of load on first span	59
24.	Maximum vertical acceleration of load on second span	60
25.	Permanent deflection of first mid-span under repeated loading	61
26.	Permanent deflection of second mid-span under repeated loading	62
27.	Variation of permanent curvature within "hinge length"	63
28.	Dynamic test record for sprung case: $\alpha = 0.05160$, $\beta = 1.2$	64
29.	Dynamic test record for sprung case: $\alpha = 0.04313$, $\beta = 1.6$	65
30.	Dynamic test record for sprung case: $\alpha = 0.05795$, $\beta = 1.6$	66
31.	Maximum deflection of first mid-span (sprung case)	67
32.	Maximum deflection of second mid-span (sprung case)	68
33.	Location of load for maximum deflection of first mid-span (sprung case)	69
34.	Location of load for maximum deflection of second mid-span (sprung case)	70
35.	Maximum compressive spring force on first span	71
36.	Maximum compressive spring force on second span	72

Figure Page

37. Location of maximum compressive spring force on first span 73

38. Location of maximum compressive spring force on second span 74

1.1. Ob

based on
gained r
in desig
theory f
theory"
literatu
work has
of struc
in this
loads,"
the stru

attracte
relation
works on
except
and Syme
of simpl
unsprung
there ha
subject

I. INTRODUCTION

1.1. Object and Scope

Since the end of World War II, structural design based on the concept of ultimate strength has increasingly gained recognition. This is evidenced by the appearance in design codes of practices based on the ultimate strength theory for reinforced concrete members, and the "plastic theory" for steel structures. Meanwhile, in the technical literature considerable analytical and experimental research work has been reported on fundamental studies of the behavior of structures beyond the elastic range. Published works in this area, however, generally deal with "stationary loads," i.e., loads that do not change their positions on the structure.

For many decades the problem of moving loads has attracted a great deal of attention because of its obvious relation to bridge engineering. However, most published works on this subject are confined to elastic behavior, except the two analytical studies reported by Parkes (1) and Symonds and Neal (2). Both works considered the response of simply supported "rigid plastic" beams subjected to an unsprung moving mass. Except for the studies by Hills (3), there has been no reported experimental work on the subject. The investigation of Hills was concerned with

the inelastic behavior of simply supported beams subjected to moving unsprung or sprung loads. Reported herein is an experimental study of the inelastic behavior of two-span continuous beams.

The experiments performed in this study consist of subjecting two-span symmetrical continuous beams to unsprung and sprung loads moving across the length of the beam. A total of 20 beams were tested in this manner. Each beam is 6 ft. long (3 ft. each span), made of mild steel, and has a rectangular cross-section of 1" x 1/4". It was loaded in the weaker direction. The parameters considered in the study are the weight and the speed of the load. The weight of the load was varied from 0.56 to 1.8 times the minimum value of a static (but movable) load that would first cause yielding in the beam. The load speed used was varied from 0.2 fps to 15.3 fps.

Quantities measured in the experiments were deflections at the centers of the two spans of the beam, and the reaction between the moving load and the beam. To aid the planning and interpretation of the dynamic tests certain static tests were also performed. These tests as well as other related to the experiment program are described in Chapter II. The results of the investigation are presented in Chapter III which is followed by a summary, and concluding remarks in Chapter IV.

1.2. Notation

The symbols used herein are defined in the text where they first appear. For convenience, the most important ones are summarized here in alphabetical order.

E = Young's modulus

g = gravitational acceleration

I = moment of inertia of the beam section

L = length of one span of the two-span beam

m = mass per unit length of beam

M = bending moment

M_u = ultimate moment capacity of the beam section

M_y = yield moment = $2/3\ M_u$

P = concentrated load

P_c = (minimum) collapse load, (see Fig. 8)

P_y = (minimum) yield load, (see Fig. 8)

T_1 = fundamental period of the two-span continuous beam

t = time

v = horizontal velocity of the load

w_s = weight of sprung part of empty carriage

W = weight of load

x = distance from the first or second support

y_c = static deflection at (first or second) mid-span

y_y = static deflection at $x/L = 0.4323$ due to P_y

α = $vT_1/2L$, speed parameter

β = W/P_y, weight parameter

II. EXPERIMENTAL WORK

2.1. Experiment Set-up

2.1.1. General. The set-up of the experiments is essentially the same as that used for a previous experimental study of simply supported beams by Hills (3). For the sake of completeness, however, the set-up will be briefly described herein along with certain necessary modifications in order to accommodate the testing of the continuous span. An overall view of the set-up except the "load arrester" is shown in Fig. 1.

2.1.2. Test Beams. (See Fig. 3.) Each test beam is 6'-0" long (3'-0" each span) having a uniform rectangular cross-section of 1" x 1/4" and loaded in the weaker direction. The specimens were cut from hot rolled mild steel (C 1095) bars (each about 20 ft. in length) rolled specially for this investigation by the Bethlehem Steel Company. The total weight of the test beam is about 5.1 lb. The elastic fundamental natural frequency of vibration is 17.7 cps. The yield stress of the material which averages about 27,500 psi will be discussed in detail in Section 2.3.1. The static behavior of the continuous beam is discussed in Section 2.4.

To facilitate adjustment for a smooth junction between the test beam and the "approach span," each end of the test beam (as well as the approach span) was beveled so that it makes an angle of 60° with the top face of the beam. At the supports, the beam is connected by set screws to "support seats" which are, in turn, attached to the "abutments" in a manner described in Ref. 3. The length of the support seat is 1" for the end support, and 1/2" for the middle support. There are elongated slots in the seats of the approach support and the middle support in order to allow horizontal movements; the seat at the third support is pinned and not allowed to undergo any translation.

2.1.3. Load Carriage. (See Fig. 2.) The load carriage consists of a load box supported by two leaf springs which are attached to a chassis bar. The springs have a combined stiffness of 181 lb. per in. One end of the bar is attached to a wheel, the other to a stabilizing bar which is connected to a monorail by rollers. The load box is restrained from horizontal motion relative to the chassis by a rod and sleeve connection, the rod being anchored at the chassis and the sleeve attached to the box. As a safety measure (in case the test beam should deflect excessively under the carriage wheel), a vertical flat bar hinged to the chassis is pin-connected to another vertical bar attached to the monorail behind the main stabilizing

bar. T
slot so
them if
slot.

number
weight
to 12.6

2.1.4.
of a 12
The weig
side the
During te
the tower
pushes th
potential
energy of

2.1.5. Lo
consists o
to a wire
across the

2.1.6. Abu
Monorails a
are made of
wide flange

bar. The pin between the two bars lies in an elongated slot so that there exists no vertical constraint between them if the pin is not in contact with either end of the slot.

The weight of the load carriage depends on the number of load plates placed in the load box. The "unsprung" weight of the carriage is constant in all tests and equal to 12.6 lb.

2.1.4. Driving System. (See Fig. 4.) The system consists of a 12 ft. tower, at the top of which is supported a weight. The weight is fastened to a wire rope which runs down outside the tower and then horizontally through several pulleys. During test, the weight is released and drops down from the tower top. An attachment on the horizontal wire rope pushes the load carriage, thus transforming most of the potential energy of the dropping weight into the kinetic energy of the carriage.

2.1.5. Load Arrester. The load arrester (see Fig. 5) consists of a pneumatic cylinder with its piston attached to a wire rope. The rope, guided by four pulleys, extends across the path of the carriage near the end of the track.

2.1.6. Abutments, Accelerating, Decelerating Tracks, Monorails and Guide Plates. (See Fig. 1.) The abutments are made of concrete blocks and short pieces of steel wide flange sections. The tracks and test beams are attached

to small brackets tied to steel plates which, in turn, are connected to the top of the wide flange steel sections. The accelerating and decelerating tracks are made of 1" x 1" square bars. The monorail is made of 1 1/2" x 1" aluminum rectangular bars supported by steel "arms" which are anchored to the web of the wide flange steel sections.

In order to ensure that the load carriage would stay on the test beam, a "guide plate" is placed along the beam (see Fig. 3). A fork-like attachment to one side of the load carriage straddles the plate as the load moves on the test beam. Rollers at the end of "fork" minimize the friction between the plate and the carriage in case they touch each other. (However, in tests they rarely did.)

2.2. Measurements and Instrumentation

The main equipment for the experimental study is a four channel Sanborn 150 Recording System (Fig. 1).

2.2.1. Beam Deflections. The deflection histories of both mid-spans are recorded by use of two Schaevitz Linear Variable Differential Transformer, type No. 4000 XS-B, with a range of $\pm$ 4".

2.2.2. Carriage Reaction. To estimate the dynamic force between the carriage and the test beam the vertical acceleration of the carriage is measured (when the leaf springs are blocked, i.e., the entire carriage behaves like an unsprung load) by use of an accelerometer (see Fig. 2).

When t
spring
record

2.2.3.
the mi
the Sa
are cl
the pa
can be

2.3. S

2.3.1.
the bea
about 2
stress
cut fro
specime
prepare

do not
For eac
specime
from th
the ord

this in

When the springs are allowed to act, the strains in the springs are measured. In either case the response is recorded by the Sanborn Recording System mentioned above.

2.2.3. Load Position. The times when the load is over the middle support and the third support are marked on the Sanborn recording paper by use of microswitches that are closed by small pieces of steel wire extending across the path of the load at the supports. The time of entry can be detected from the record of other transducer outputs.

2.3. Stress-Strain and Moment-Curvature Relations

2.3.1. Stress-Strain Relation. As mentioned previously, the beams used in this study were prepared from steel bars about 20 ft. long. In order to determine the yield stress of the material, three tension test specimens were cut from each bar. The average yield stress of these specimens is used as the yield stress for the test beams prepared from the bar.

The values of the yield stress of the specimens do not vary appreciably. They average around 27,500 psi. For each bar, the difference of the yield stress of any specimen from the average value of the three specimens from the same bar is less than 4.2%; generally, it is on the order of 2%.

A total of 76 tension specimens were tested for this investigation. The specimens are 10 1/2" long and,

for convenience, have the same constant cross-section as the bar, i.e., 1" x 1/4". Some of the results obtained by use of these specimens were compared with those obtained by use of specimens having the same shape as the ASTM standard tension coupon. Four pairs of specimens, each prepared from the same bar were tested for this purpose. The yield stress indicated by the specimens with the constant cross-sectional area was found to be a little lower than that recorded for the standard specimens. The difference, however, is small and less than 1.5%.

The yield stress was taken to be the apparent stress at which the load on the test specimen first began to drop. The speed of the moving part of testing machine was 4×10^{-4} in./sec. Shown in Fig. 6 is a typical stress-strain diagram for the material used in this study.

2.3.2. Moment-Curvature Relation. In Fig. 7 is shown the moment-curvature diagram obtained from a simple beam test as illustrated in the figure. The moment was computed from the loading on the beam. The curvature was calculated from the strains at the top and bottom faces of the beam measured by means of SR-4 strain gages.

The yield moment was computed from the loading at which the strains of the beam began to "flow." For the case shown in the figure, it is equal to 301 in.-lb., while computed from the usual beam theory and using the yield stress from the tension test, the yield moment is

292 in.-lb. The ultimate moment was computed from the load at which the deflection of the beam began to increase rapidly. It is equal to 448 in.-lb. as against the theoretical value of 438 in.-lb. based on the usual theory of plasticity using the experimental yield stress.

The "simple beam" test depicted above was repeated using a different beam. The results obtained are not appreciably different from those shown in Fig. 7.

2.4. Static Behavior of Continuous Beam

2.4.1. Theoretical Analysis. It seems natural to consider the static behavior of the structure as a basis for discussion of its dynamic behavior. In this section, certain important properties of the static response of a two-span symmetrical and continuous uniform beam to a single movable concentrated load is discussed. The beam is assumed to be made of material having an ideal elasto-perfectly plastic stress-strain relation. The cross-section is rectangular. The analysis is based on the usual theories of elastic and plastic analysis of structures.

In Fig. 8 are plotted the "yield load" and "collapse load" of the beam as functions of the position of the load (due to symmetry, only one span is shown in the figure). The "yield load" is the load at which the maximum stress in the beam just reaches the yield stress.

The maximum stress or bending moment occurs at the point where the load is applied. The yield load is

thus obtained by setting the (elastic) bending moment at the section under the load equal to the yield moment, $M_y = \frac{2}{3} M_u$, where M_u is the ultimate moment of the cross-section. The "collapse load" is the load at which the beam becomes a mechanism with one plastic hinge under the load and another over the middle support.

It is seen that the yield load is a minimum when the load is at $x/L = 0.4323$, in which x is the distance measured from the first support and L is the length of one span. Subsequently this minimum load, which will be denoted by P_y and has a magnitude of $3.2148\ M_u/L$, will be simply referred to as the "yield load," and used as a measure of the weight of the moving load. Similarly, the minimum collapse load which is equal to $5.827\ M_u/L$ and occurs at $x/L = 0.4142$, will be simply referred to as the "collapse load" and denoted by the symbol P_c. The value of the ratio of the collapse load to the yield load is 1.8125.

Fig. 9 shows a plot of the elastic deflection at the point under the load as a function of the position of the load. The maximum value is equal to $0.01509 \frac{PL^3}{EI}$ with the load at $x/L = 0.4620$. At $x/L = 0.4323$, and $x/L = 0.5$, the deflections are equal to 0.01493 and 0.01497, respectively, times $\frac{PL^3}{EI}$. Subsequently, the quantity of y_y, the deflection at $x/L = 0.4323$ for $P = P_y$, will be used as a measure of the dynamic deflections. For the beams used in the tests, the average value of y_y is 0.684 in.

2.4.2. Experimental Behavior. A static loading test of a continuous beam is depicted in Fig. 10. The load, applied gradually at $x/L = 0.4323$, is plotted against the maximum strains recorded for the section under the load and that over the middle support.

The observed yield load corresponds to the load at which the observed strains began to increase rapidly. The "theoretical" values were computed as explained in the preceding section.

It is of interest to note that while the theoretical P_y is only slightly larger than the observed P_y (35.2 lb. versus 34.8 lb.), the observed P_c is appreciably larger than the theoretical P_c (76 lb. versus 63.7lb.). The latter difference can be attributed to the strain-hardening behavior of the real moment-curvature relation versus the ideal elasto-perfectly plastic relation used in computing the theoretical value. The strain-hardening behavior is also evident in the load-strain curve for the point under the load.

The above test was repeated for another beam; the results obtained showed no significant difference from those described in the preceding.

2.5. Test Program

2.5.1. Parameters of Study. In this investigation there are essentially two parameters: the weight (W), and the speed (v) of the load. In the subsequent description of

the t

these

dimens

in whi

beam,

the la

the la

W in 1

paramet

springs

2.5.2.

ranging

0.002 t

15.3 fp

g genera

g--from

of the

discusse

used in

of g.

the test program and the presentation of the test results, these parameters are made dimensionless. The corresponding dimensionless parameters are:

$$\alpha = \frac{vT_1}{2L} \doteq 0.00941\ v \tag{1}$$

$$\beta = \frac{W}{P_y} \doteq 717\ W/\sigma_y \tag{2}$$

in which T_1 denotes the fundamental elastic period of the beam, and σ_y is the yield stress of the beam material. In the last expression in Eq. (1), v should be in fps; in the last expression of Eq. (2) σ_y should be in psi and W in lb.

Note that for the sprung load tests, no additional parameter presents itself as there was only one set of springs used in the tests involving sprung loads.

2.5.2. Unsprung Load Tests. Nine values of β were used ranging from 0.56 to 1.8. Values of α used ranged from 0.002 to 0.1442 (corresponding to speeds from 0.2 fps to 15.3 fps). The number of speeds used for each value of β generally decreases with an increase in the value of β--from 7 for $\beta = 0.56$, to 2 for $\beta = 1.8$. Also, because of the "jump" phenomenon occurred in the test and to be discussed later, the maximum value of the load speed used in the test is generally smaller for larger values of β.

2.5.3. Sprung Load Tests. Four values of β were used ranging from 0.6 to 1.6. The α values used ranged from 0.002 to 0.1315 (corresponding to speeds from 0.2 fps to 14.0 fps).

III. RESULTS OF INVESTIGATION

3.1. Unsprung Loads

3.1.1. Typical Patterns of Behavior. From the test data obtained, there were seen four distinct patterns of behavior of the load-beam system as affected by the speed parameter α and the weight parameter β. These patterns are discussed below.

3.1.1.1. Behavior with "Medium" Value of α and "Medium" Value of β. In Fig. 11 is shown the test records for the case of a "medium" value of α (= 0.05623) and of β (= 1.0). It should be noted that the terms: "medium," "small," and "large" are used here and subsequently only in a qualitative sense to facilitate the presentation.

The three vertical lines in Fig. 9 mark the times when the load was at the first, second, and last support, going from left to right. The average speed of the load on the first and second spans, computed from these times, are 6.12 fps and 5.83 fsp, respectively. The top trace represents the time history of the vertical acceleration of the moving load; a downward acceleration is above the datum line. The reaction on the beam is, of course, directly proportional to this acceleration. Hence, the acceleration trace may be regarded also as the reaction trace.

It is seen that there is little variation in the acceleration except when the load is near the second and the third supports. At these locations, the deformations of the beam are relatively insensitive to variations in the interaction force. The maximum acceleration were 0.641 g and 1.396 g for the first and second span, respectively.

The second trace represents the deflection history of the mid-point of the first span. The maximum static deflection of this point, computed on the basis of perfect elasticity and the load applied statically at the same point, is marked by a horizontal line in the figure. It is seen that the maximum dynamic deflection is approximately 30% larger than the static. After the load has passed the test beam, this point exhibits a fairly regular harmonic and slightly damped motion in the first natural mode. There was no permanent deflection.

The third trace represents the deflection history of the mid-point of the second span. In this case, the maximum dynamic deflection is also about 30% larger than the maximum static. No permanent deformation could be detected in this test.

3.1.1.2. Behavior with "Small" Value of α and "Large" Value of β. In Fig. 12 are shown the test records for the case $\alpha = 0.04468$ and $\beta = 1.6$. The general patterns of the response curves are similar to those shown in Fig. 11. In particular, it may be noted that the reaction on the

beam, as seen from the acceleration trace, did not vary substantially (except near the supports). The behavior in this case, however, differs from the preceding one in the occurrence of permanent sets or deformations. It is of interest to note that the permanent set of the first span is 0.053 in. while that of the second span is 0.018 in. only. These sets are actually relatively small--less than 8% of the yield deflection y_y. This difference is thought to be due to two reasons: (1) the influence of residual bending moments, and (2) the influence of decreased load speed in the second span.

For this particular case, the beam may be thought of as being subjected to a heavy load first at the center portion of the first span; the load was then taken off and placed on the center portion of the second span. (Note that from the acceleration records, the magnitudes of these loads were about the same.) Because of the large magnitude of the load, when the load is at the first span, inelastic action takes place in the beam, and the second span would be called upon to take on a larger negative bending moment than that would be required if the response were completely elastic. (See Fig. 13(a)). Upon unloading--the load moves toward the middle support--a distribution of negative "residual" bending moment would exist in the beam as shown in Fig. 13(b).

As the load goes near the center portion of the second span, it causes positive bending moment in this

span. In order for inelastic action to take place, the residual negative moment would have to be overcome first. Hence, the beam would appear stronger in the second span. This would explain, at least in part, why the permanent deformation in the second span is smaller. The other reason for this smaller damage is the fact that when the load came on the second span, its speed had been decreased, and small speeds seem to cause smaller dynamic effects. A difference in the magnitude of accelerations, though small, can be seen from the top trace of the record.

For this type of behavior, the shape of the final deformed beam could appear as that depicted either by Fig . 14(a) or (c), depending upon how large β was. In Fig. 14, a "hinge" represents a noticeable region of permanent deformation or curvature. The "hinge" actually has the shape of a smooth "bow," and its characteristics are considered in Section 3.1.7. for several typical cases. It should be noted also that the "hinge" over the middle support usually represents an yielding of appreciably smaller magnitude as compared to the yielding of the mid-span points. In some cases, it is hardly noticeable.

3.1.1.3. Behavior with "Medium" Value of α and "Large" Value of β. In Fig. 15 are shown the test record for the case $\alpha = 0.06108$ and $\beta = 1.6$. The behavior in this case is quite different from the preceding ones. As the load enters the beam there is a downward acceleration, signifying

a smaller reactionary force than the static. But the acceleration rapidly becomes upward with a maximum value of 0.612 g (signifying that the reactionary force is 1.612 times the static load) that occurs when the load is approximately at the two thirds point of the first span. Then it suddenly turns downward with a magnitude of one g. This indicates that the moving load has lost contact with the surface of the beam or has "jumped." The period during which the acceleration remains constant at one g is the duration of the load "in the air." This period covers the interval from approximately 1/5 of the span length to the left of the middle support to approximately 1/10 of the span length to the right of the middle support. As the load lands on the second span there would, of course, be an impact as evidenced by the large and rapid variations of the acceleration. After the load stabilizes itself, the pattern of acceleration becomes similar to that when the load was on the first span.

The phenomenon described in the preceding is also reflected in the deflection traces in Fig. 15. It is seen that when the load is in the air, the beam vibrates freely. In contrast to the previous case, the permanent set in the second span is larger than that in the first span (0.109 in. versus 0.035 in.). This may be explained by the "jump" phenomenon and the associated impact effects.

The maximum dynamic deflection in this case is larger than the maximum static deflection by 47%, and 46%,

respectively, for the first and second spans.

The shape of the final deformed beam may appear either as that shown in Fig. 14(b) or 14(c).

3.1.1.4. Behavior with "Large" Value of α and "Medium" Value of β. In this case the jump phenomenon as described in the above section also takes place. A permanent displacement is usually seen in the second span, and the final shape of the deformed beam appears as that shown in Fig. 14(b). The hinge at the middle support may or may not be formed.

3.1.2. "Jump" Phenomenon. The jump phenomenon brought out in the preceding section has been noted also in test records for other combinations of the values of α and β. Although the phenomenon appears interesting, to study the behavior of the system involving such a phenomenon would seem to have questionable practical significance, as it is a moot point, for example, whether a vehicle should be knowingly allowed to jump on a bridge and cause an impact. Nevertheless, it is deemed significant to mark the critical combinations of the values of the parameters at which a jump would first occur. This information is shown in Fig. 16. It is seen that jump would occur when the value of either α or β, or both, are large.

It may be noted that in order to verify the occurrence of a jump, in some tests a piece of thin white paper was placed over a piece of thin carbon paper which was

attached to the beam. As the load moves on the beam, the reaction marks on the paper an impression with an intensity varying according to that of the pressure. The jump phenomenon is seen by noting a gradual fading and then a complete disappearance of any trace of carbon on the paper. The subsequent landing impact of the load after the jump is manifested by the intense coloring of the white paper.

Although the phenomenon can be observed, it does not seem feasible to explain it fully. If the load is in contact with the beam, then the following relation holds:

$$\frac{d\bar{y}}{dt} = \frac{\partial y}{\partial t} + v \frac{\partial y}{\partial x} \tag{3}$$

in which $\frac{d\bar{y}}{dt}$ is the vertical velocity of the load, $\frac{\partial y}{\partial t}$ is the (local) vertical velocity of the beam, and $\frac{\partial y}{\partial x}$ the instantaneous slope of the beam. For a given time the value of the right-hand side of the equation is fixed. The actual value of $\frac{d\bar{y}}{dt}$ depends on the load trajectory which of course is influenced by all the variables that enter into the problem. A jump occurs when the value of $\frac{d\bar{y}}{dt}$ is larger than that of the right-hand side of the equation.

In Fig. 17 are plotted, for various values of β, the location at which the load leaves the (first) span as a function of α. It is seen that, for $\beta < 1.2$, this location in general moves closer to the middle support with increasing values of α. However, such is not the case

for large values of β. It may be noted that the range within which this location varies is not large: 0.83 L to 0.98 L.

3.1.3. Maximum Mid-Span Dynamic Deflections. The maximum dynamic (downward) deflection of the first mid-span is plotted in Fig. 18, as a function of α for various values of β. Almost all curves indicate a trend of increasing deflections with an increase in the value of α. Furthermore, the larger the value of β, the greater the rate of the increase. The exception concerns the case with the heaviest load: $\beta = 1.8$. In this case the relative large deflection at a very low speed is thought to be due to the longer time available for the inelastic deformation to take place.

The "jump line" as depicted in Fig. 16 is reproduced in this figure also, indicating that the results to the left of the line correspond to tests that did not involve a jump, and those to the right correspond to tests in which the jump phenomenon was observed. However, it should be noted that in this case the maximum deflection plotted generally occurred before the jump did take place. Such is not the case for the maximum mid-span deflections in the second span which are plotted in Fig. 19.

The data in Fig. 19 show the same general trends as those in Fig. 18. However, the increases in the deflections involving the jump phenomenon, as expected, are much larger, since a jump affects the second span response to a much

greater extent than the first span response. It is also noted that, unlike the case for the first mid-span deflection, the second mid-span deflection for $\beta = 1.8$ at the lowest speed is smaller than that at the next higher speed. This is thought to be due to the existence of the residual bending moments set up by the yielding in the first span as explained in Section 3.1.1.3.

In Fig. 20 is plotted the distance between the location of the moving load and the first support when the maximum first mid-span deflection occurred. This distance varies within a region from 0.4 L to 0.75 L. For the case of a single static load and a perfectly elastic beam, it is 0.4620 L. (See Fig. 9.) In general, an increase in α results in a larger value for this distance.

Similarly the distance from the second support to the position of the load at which the maximum second mid-span deflections occurred is plotted in Fig. 21. The trend is similar to that shown in Fig. 20. But for large values of α, the results become somewhat erratic due to the occurrence of the jump phenomenon.

3.1.4. Mid-Span Permanent Deflections. The permanent deflections of the first and second mid-spans are plotted in Fig. 22. Downward deflections are shown positive. It should be noted that these permanent deformations are taken after the load has crossed both spans. Because of the anti-symmetrical mode of the deflection curve, the

permane

to offs

β = 1.

small, h

there is

span at

discussi

longer t

heavy loa

was cause

span yiel

second sp

strengthe

previousl

A

the dynam

resulting

span and s

3.1.5. Ma

accelerati

in Fig. 23

acceleratio

ordinate re

load over th

It i

permanent deformations at the first and second spans tend to offset each other.

Therefore, except for the heaviest load considered, $\beta = 1.8$, the magnitudes of the permanent sets are quite small, being only a small fraction of y_y. For $\beta = 1.8$, there is a relatively large permanent set in the first span at the lowest load speed. As mentioned in the previous discussion of maximum deflections, this is because of the longer time available for the beam to yield under the heavy load. The negative permanent set of the second span was caused by the uplifting that occurred when the first span yielded under the load; the subsequent loading of the second span did not offset this uplift on account of the strengthening effect of the residual moment as described previously.

At higher speeds and with the occurrence of jumps, the dynamic effects in the second span became dominant resulting in large positive permanent sets in the second span and smaller negative sets in the first span.

3.1.5. Maximum Acceleration of Load. The maximum vertical acceleration of the moving mass on the first span is plotted in Fig. 23. The acceleration is scaled by the gravitational acceleration g. Thus, for a given β value, the vertical ordinate represents the maximum increment of the dynamic load over the static load in terms of the static load.

It is seen that, for tests that did not involve a

jump, this increment is less than unity. For those involving a jump (at higher values of α) the increment can attain values as high as two. However, it should be noted that, in general, these maximum accelerations actually occurred before the jumps took place. The point with an acceleration of 2.6 g at $\alpha = 0.0775$ is an exception. In this case the load jumped and landed also on the first span; this resulted in the relatively large values of acceleration.

Similarly shown in Fig. 24 is the maximum acceleration of the load on the second span. The values of the acceleration are generally larger than those in the first span. For cases involving no jump, the maximum value is 2 g; for cases involving a jump, the maximum value reaches 4.6 g. In the latter cases, of course, the high values were associated with the impact on the second span after the jump.

3.1.6. Deformation Under Repeated Loading. In Fig. 25 are plotted for a number of test beams the accumulated permanent set of the first mid-span under repeated loading. In each case the static magnitude and the speed of the load were kept the same.

It is observed that the permanent sets either increase or decrease monotonically with the number of load applications. The case of increase is associated with large values of β, while that of decrease with smaller values of β and usually at high values of α.

This can be explained by the observation already made in Section 3.1.1. In the case of large values of β, the first span suffers a greater amount of damage than the second span. For smaller values of β and at high speeds, the negative permanent sets are really caused by the downward permanent deformation in the second span resulting usually from the jump phenomenon.

Similar data are shown in Fig. 26 for the accumulated permanent set in the second mid-span. In this case, the deformations all increase with the number of applications of the loading.

It is noted from both Fig. 25 and Fig. 26 that as the number of applicationsincreases, there is no sign that the beam would "stabilize" in the sense that the increase in deformation per application would become smaller. However, it must be pointed out that the number of applications considered in the data is very small, with six as the maximum. Such stabilization might take place with a larger number of applications for cases having smaller values of β.

For the case of repeated loading, measurements were also recorded of the maximum mid-span deflections and the slopes of the beam at the two end supports. These data indicate similar trends to those mentioned above for the permanent sets; hence, they are not presented here.

3.1.7. Permanent Curvature and "Hinge Length." In this section the permanent curvatures of the "hinges" in six

beam specimens are studied. The term "hinge length" denotes the distance interval within which permanent curvatures are noted. (An end of a "hinge" is marked by the point at which the beam begins to deviate from a straight line.)

In Fig. 27 is plotted the distributions of the permanent curvature along the hinge length for different specimens. (The curvatures were obtained from the displacements by use of finite difference expressions for which a difference interval of 1/7 of the hinge length was used.) Although the distribution is not symmetrical, in each case there is only one maximum peak value. It may be noted that by comparing with the bending moment-curvature graph shown in Fig 7, the numerical value of these maximum curvature would appear to be quite reasonable.

In Table 1 are listed additional data on the "hinges" for the six specimens. In this table the term "angle change" represents the angle between the tangents at the two ends of the hinge, and "average curvature" is obtained by dividing the angle change by the hinge length.

It is seen that generally the hinge length is shorter in specimens used in dynamic tests than in static tests. The shortest hinge (specimen S-22-2) corresponds to a sprung load case which is to be discussed in the next section. It is of interest to note that, for this case the value of α is the largest of the cases considered, and the distribution of curvature shows the sharpest and highest

Table 1. "Hinge length" and permanent curvature.

Specimen No.	β	α	"Hinge Length"	Number of of Applications	Sprung or Unsprung Case	Max. Curvature ($\times 10^{-2}$)	Total Angle Change (rad.)	Average Curvature ($\times 10^{-2}$)
S-13-2	1.0	0.09040	3-15/16"	4	Unsprung	3.600	0.1134	2.875
S-6-2	1.2	0.08073	5-1/8"	2	Unsprung	3.725	0.1850	3.600
S-22-2	1.2	0.09340	3-3/4"	1	Sprung	10.000	0.1108	2.950
S-17-2	1.4	0.07435	6-3/4"	4	Unsprung	1.775	0.0951	1.410
S-11-2	1.8	0.04065	5-1/8"	4	Unsprung	2.675	0.1029	2.000
PT-4	(Static Test)		6-1/8"	--	--	4.500	0.1239	2.025

peak among the curves in Fig. 27. In terms of span length, the hinge length varies from 1/10 to 1/5. The maximum curvature varies from 1.775×10^{-2} to 10×10^{-2} rad./in. and the average curvature varies from 1.40×10^{-2} to 3.60×10^{-2} rad./in.

3.2. Sprung Loads

3.2.1. Typical Patterns of Behavior. In order to gain some insight into the behavior of the beam-load system considered, three typical test records are presented and discussed in the following. It should be noted that in all the sprung load tests, included in the value of β there is a constant fraction approximately equal to 0.32 that corresponds to the unsprung portion of the load carriage. The natural frequency of the sprung load, of course, varies with the value of β. It is on the order of 6 cps, or about 1/3 of that of the unloaded beam. Damping in the load system is not significant.

3.2.1.1. Behavior with "Medium" Value of α and "Medium" Value of β. Shown in Fig. 28 are the test records for the case: $\alpha = 0.0516$ and $\beta = 1.2$. The top trace represents the vertical acceleration of the unsprung portion of the load. In contrast to the unsprung case, this acceleration curve oscillates a great deal. However, if a mean curve is passed through the oscillations, a trend can be discerned that is similar to the unsprung case shown in Fig. 11.

The magnitude of the acceleration is rather small, on the order of one third of g corresponding approximately to 0.1 P_y. Hence, its influence on the total reactionary force is relatively small.

The second and third traces, as before, represent the deflection histories of the mid-points of the first and second spans. The maximum dynamic deflections are 38% and 21% greater than the static ones for the first and second spans, respectively.

The trace at the bottom represents the variation of the total force in the springs of the carriage. The datum line represents the static value. An upward excursion of the trace denotes a decrease in the reaction on the beam. As expected, as the load first enters the beam, the downward displacement of the beam causes a decrease in the spring force. The subsequent behavior of the spring force is governed by the complex interactions of the two mechanical systems: the beam and the carriage. Near the first mid-span there is a relative maximum increase of sprung force of 12.6 lb. (approximately 1/3 P_y). A similar relative maximum in the second span amounts to about 1/4 P_y only. This is in agreement with the observation that the maximum mid-span deflection of the first span is appreciably larger than that of the second span.

No permanent set or distortion is seen for this test.

3.2

Valu

a =

simi

feat

is a

magni

The m

than

respe

the m

respec

deform

is ill

3.2.1

Value

a = 0.

that t

surfac

This m

val as

the cas

load, t

varies

the spri

3.2.1.2. Behavior with "Small" Value of α and "Large" Value of β. Figure 29 shows the test records for the case $\alpha = 0.04313$ and $\beta = 1.6$. Qualitatively, these records are similar to those shown in Fig. 28. The distinguishing feature of the test recorded in this figure is that there is a permanent set in the first span, though it is small in magnitude. There is no permanent set in the second span. The maximum mid-span deflections are 49.7% and 19.6% larger than the static values for the first and second spans, respectively. The maximum increases in spring force near the mid-span correspond approximately to 0.45 P_y and 0.33 P_y, respectively, for the first and second span.

For this type of behavior, the final shape of the deformed beam is similar to that in the unsprung case, and is illustrated in Fig. 14(a) or (c).

3.2.1.3. Behavior with "Medium" Value of α and "Large" Value of β. This case is illustrated in Fig. 30 for $\alpha = 0.05795$ and $\beta = 1.6$. The feature of this result is that the carriage has "jumped," or lost contact with the surface of the beam, in the vicinity of the middle support. This may be seen by noting the free vibration in that interval as indicated by the two beam deflection traces. Unlike the case involving the jump phenomenon for an unsprung load, the acceleration trace does not remain constant but varies somewhat. This is probably due to the presence of the spring force. The spring force, in this case, does

not var

contras

vicinit

was inv

first s

displac

load cr

the equ

interva

permane

(about

of the

load.

span.

and neg

the sub

enters

explain

passed

oscilla

to note

unsprun

of the s

the shoc

not vary appreciably in the interval of jump; this is in contrast with the large variation of spring force in the vicinity of the middle support for cases in which no jump was involved.

The maximum dynamic mid-span displacement in the first span is 60% larger than the static. The permanent displacement had been 0.296" (about 0.43 y_y) before the load crossed the second span. This value was estimated from the equilibrium position of the free vibrations in the jump interval. After the load crossed the second span, the permanent set of the first span decreased to 0.166" (about 0.24 y_y). This, of course, is due to the uplifting of the first span when the second span yielded under the load.

There is no net permanent deformation in the second span. The reason lies in the upward permanent deflection and negative residual moments in the second span caused by the substantial yielding of the first span before the load enters the second span. A similar situation has been explained in Section 3.1.1.2.

The end of the jump, coming shortly after the load passed over the middle support, is marked by the violent oscillations in the acceleration trace. It is of interest to note that, in this case in contrast to the case of unsprung loads, the impact did not result in large response of the second span. This is thought to be due mainly to the shock-absorbing influence of the carriage springs.

The final shape of the deformed beam may appear as that shown in Fig. 14(c) with or without the hinge over the middle support.

3.2.1.4. Behavior with "Large" Value of α and "Medium" Value of β. In this case the jump phenomenon as described in the unsprung case and above section also occurs. The final shape of the beam appears as that shown in Fig. 14(b) with or without the hinge over the middle support.

3.2.2. "Jump Line." As was done for the case of the unsprung load tests, a "jump line" indicating the combinations of the values of α and β at which jump would first take place is plotted also in Fig. 16. It is seen that this line lies very close to that for the unsprung load tests.

3.2.3. Maximum Mid-Span Dynamic Deflections. The maximum deflection of the first mid-span is plotted in Fig. 31. The trend seen from these curves is similar to that noted in the case of the unsprung load tests; that is, the deflection increases with an increase in α. However, at higher values of α, the rate of increase becomes smaller, even suggesting a tendency of decreasing deflections had the values of α been increased further.

Similar data for the second mid-span are shown in Fig. 32. The large deflections to the right of the jump line are, of course, caused by the impact resulting from the jump. The location of the moving load when the maximum

deflection occurs is plotted in Fig. 33 and 34 for the two mid-spans. Likewise, the data are similar to those described previously for the unsprung load tests.

3.2.4. Maximum Spring Force. The maximum compressive spring force, in terms of w_s, which denotes the static weight of the sprung part of the carriage for $\beta = 0.56$, is plotted as a function of α for various values of β in Figs. 35 and 36 for the first and second span, respectively. The data indicate that the spring force increases as α increases. For larger α values, the maximum spring force at the second span increases faster than that at the first span with an increase in α.

Fig. 37 shows the location of the maximum spring force at the first span. The location in general moves toward the middle support with an increase in the value of either α or β. For small values of α, the location is near the point $x = 0.46\ L$ for all the data presented. An exception to the above trend occurs for values of α close to 0.05 and larger values of β. In this case, the maximum spring force occurs at the middle support. The location of the maximum spring force in the second span is shown in Fig. 38. The data appear erratic on account of the jumps of the carriage involved.

IV. SUMMARY AND CONCLUSION

4.1. Summary

An experimental study of the elasto-inelastic behavior of two-span continuous beams subjected to moving loads has been reported. The variables of the study have been the speed parameter α and the weight parameter β. In the study the value of α was varied from 0.002 to 0.1442 (0.2 fps to 15.3 fps), and the value of β from 0.56 to 1.80 (0.56 to 1.8 times P_y, the minimum yield load). The typical patterns of behavior observed are summarized as follows.

(1) For medium values of α and β, the load moved smoothly over the beam. Although the dynamic deflection was appreciably larger than the static deflection, there was no permanent set.

(2) For a small value of α and a large value of β, the load also moved smoothly over the beam. Permanent deflections were observed. The permanent deflection of the first span was larger than that of the second span. This is thought to be due largely to the negative residual moment set up in the beam as a result of the yielding in the first span.

(3) For a medium value of α and a large value of β, the load "jumped" off the beam as it approached the middle support. Then it "landed" on the second span at a short

distance beyond the middle support. The resulting impact on the second span caused relatively large deflections and permanent sets, particularly at the (second) mid-span.

(4) For a large value of α and a medium value of β, the behavior is similar to the preceding case, but usually there was no permanent set in the first span.

The maximum permanent deflections observed were actually small in magnitude. If no jump had occurred in the test, they were on the order of 0.1 to 0.3 of y_y. If jump had occurred, the permanent deflection could be much larger. However, for each load weight, the value of the maximum load speed used was limited by the jump phenomenon in the sense that the maximum speed used was only slightly larger than the speed at which jump was first observed.

A limited study on the effects of repeated loading showed that there was no stabilization of the permanent deflections after a few cycles of loading. A study of the length of the region of yielding, or the "plastic hinge length," indicates that it may vary from 1/5 to 1/10 times the span length. Except for the mitigatory effect of the load springs on the impact after a jump, for the data obtained, there is no marked difference in the general trends of behavior between the tests using sprung loads and unsprung loads.

4.2. Discussion and Conclusion

Perhaps the most prominent phenomenon observed in the experiments is the "jump." Because of the impact involved in the phenomenon, it changes the nature of the problem. As mentioned previously, the significance of a study of the beam response involving an impact of this type seems of questionable engineering significance, as it is a moot point, for example, whether a vehicle should be knowingly allowed to jump on a bridge.

On the other hand, it seems worthwhile to know the combinations of the parameters at which such a jump would occur. In this connection, it may be noted that a jump would occur at either a heavy load or a high speed. As the load is made heavier, the speed at which a jump first takes place decreases. Thus, if the jump is not allowed to happen, then it would seem that the maximum load that could pass the beam could not be much larger than the static collapse load. However, it is noted that at $\beta = 1.8$ (the static collapse load corresponds to $\beta = 1.8125$), the load can still cross the beam with a permanent set less than y_y.

As possible topics of future investigation, it is suggested that, first, an analytical study be made to compare with the experimental work reported herein, and secondly, the problem of multiple axle loads be considered. It could happen that due to a distribution of the total load, higher speeds might be attainable without the

occurrence of a jump. This, in turn, could raise the upper limit of the total weight of the load that can cross the beam.

LIST OF REFERENCES

(1) Parkes, E. W., "How to Cross an Unsafe Bridge," Engineering, Vol. 186, November, 1958.

(2) Symonds, P. S., Neal, B. G., "Travelling Loads on Rigid-Plastic Beams," Journal of Engineering Mechanics Division, ASCE, Vol. 86, No. EM1, January, 1960.

(3) Hills, R. E., "Inelastic Behavior of Simple Beams Subjected to Moving Loads," M.S. thesis (in preparation), Department of Civil Engineering, Michigan State University.

FIGURES

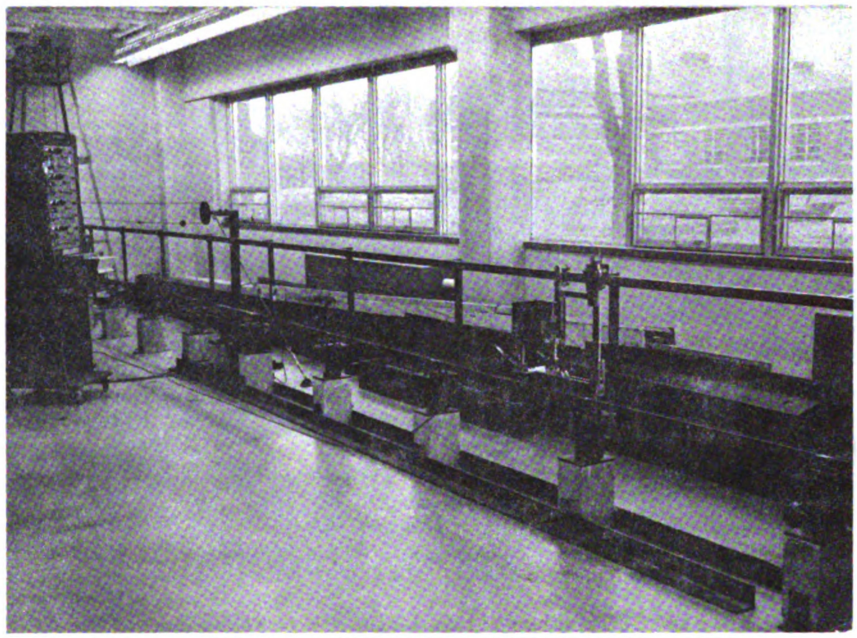

Figure 1--Overall view of test set-up.

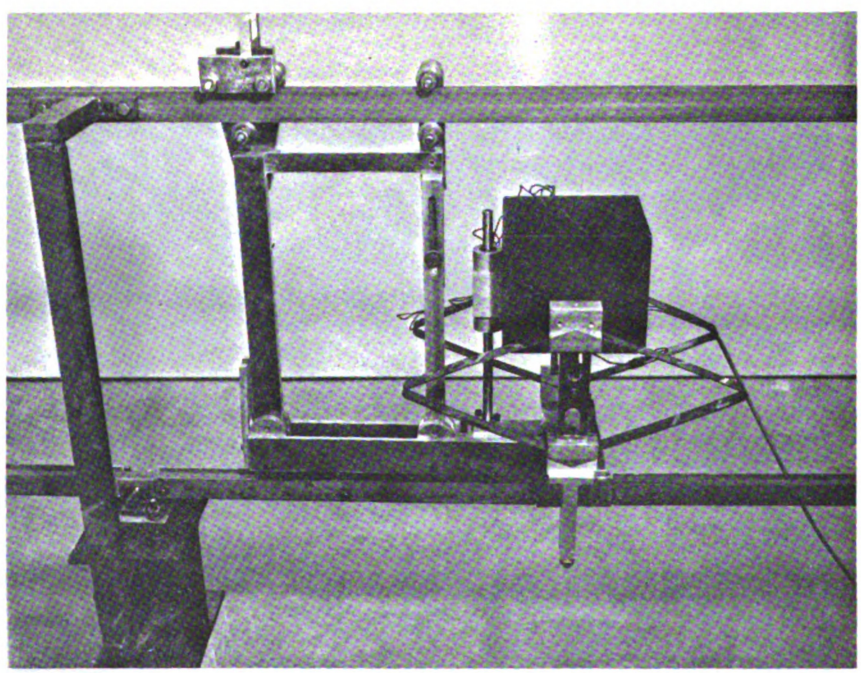

Figure 2--Load carriage.

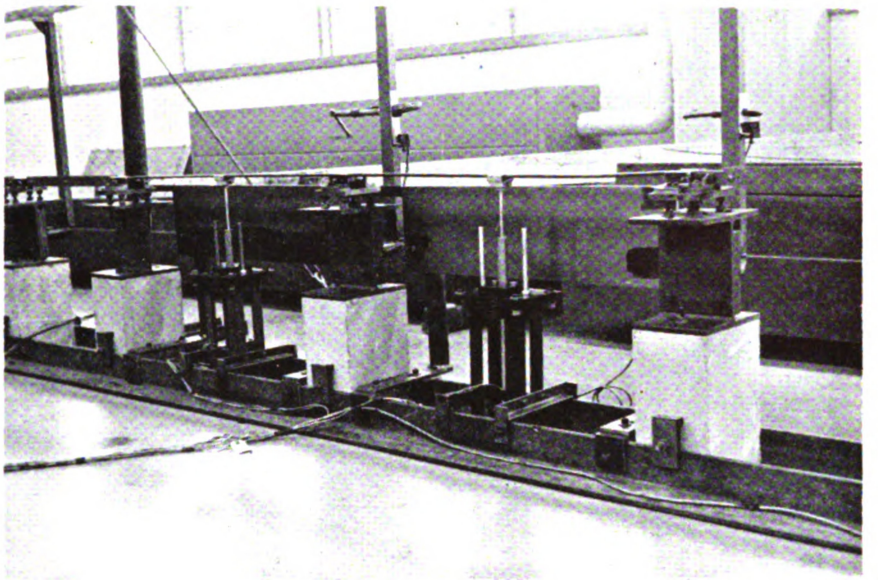

Figure 3--Test beam and differential transformers.

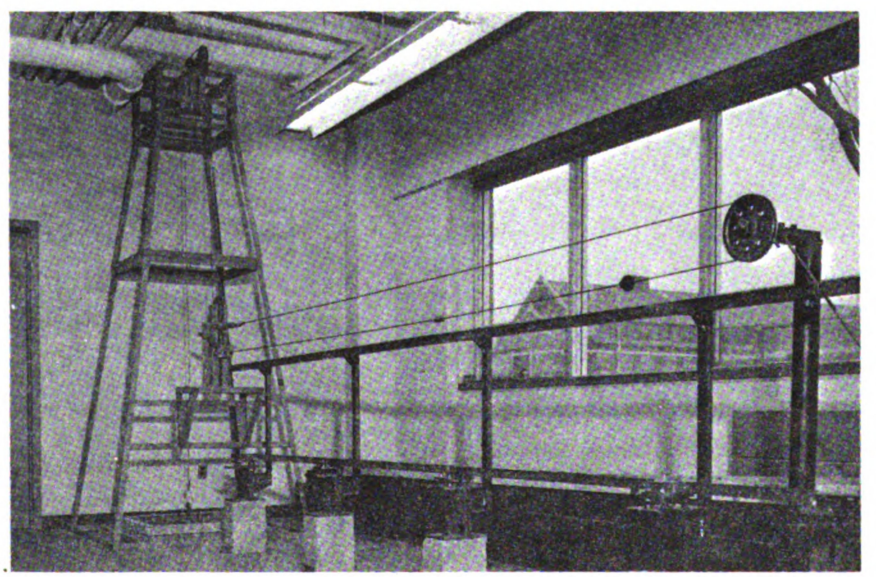

Figure 4--Driving system.

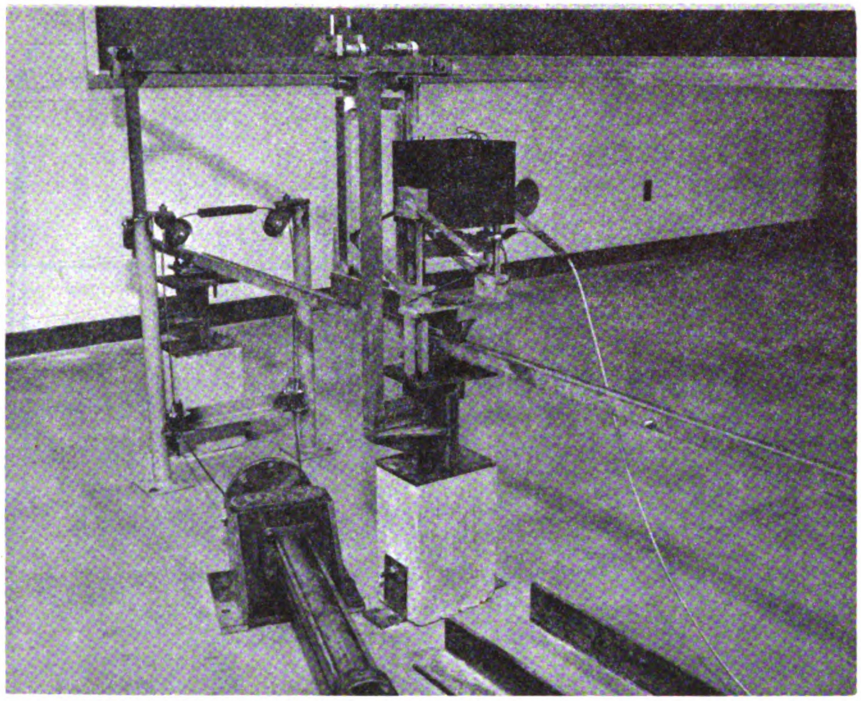

Figure 5--Load arrestor.

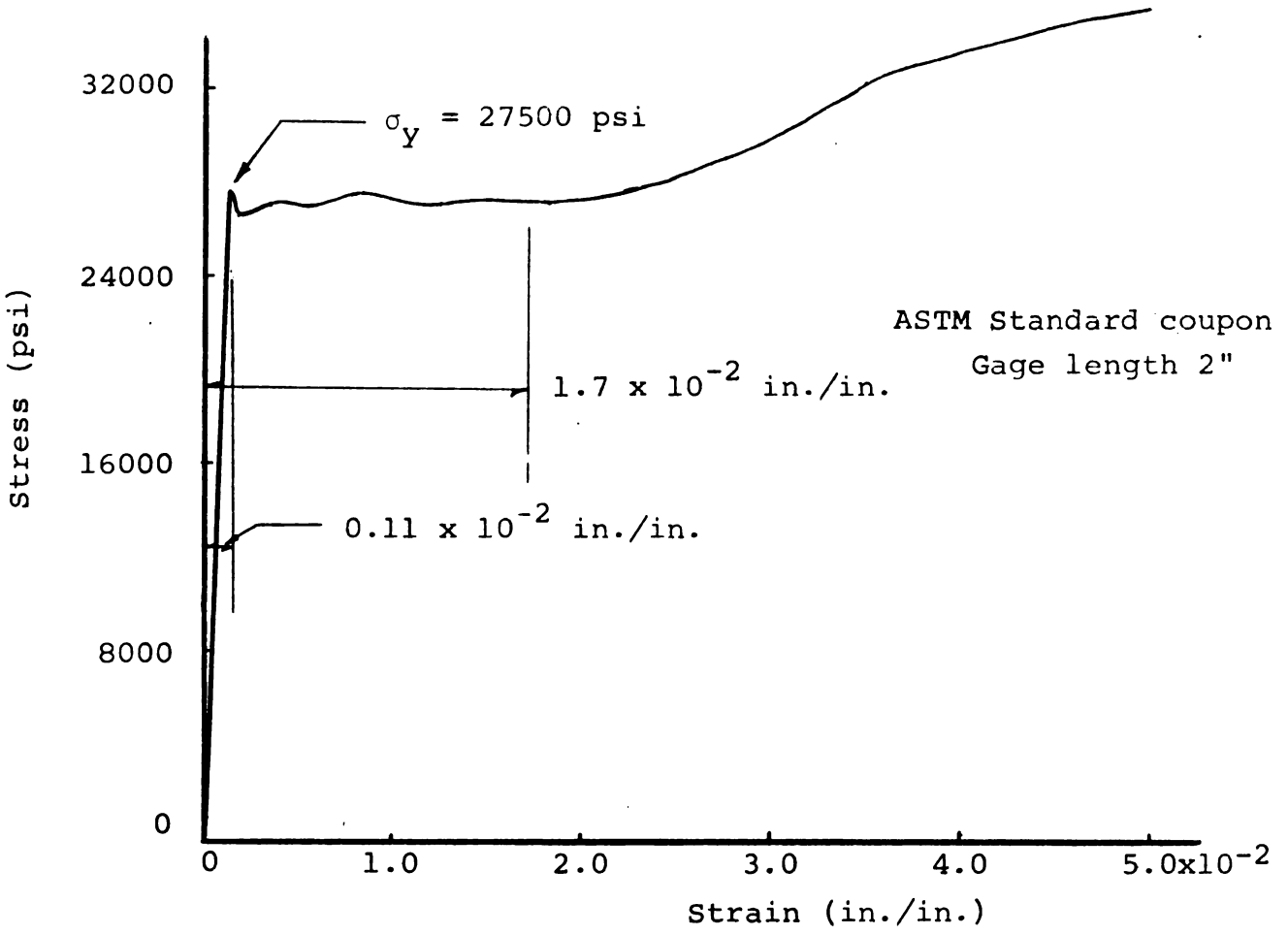

Figure 6.--Typical stress-strain curve.

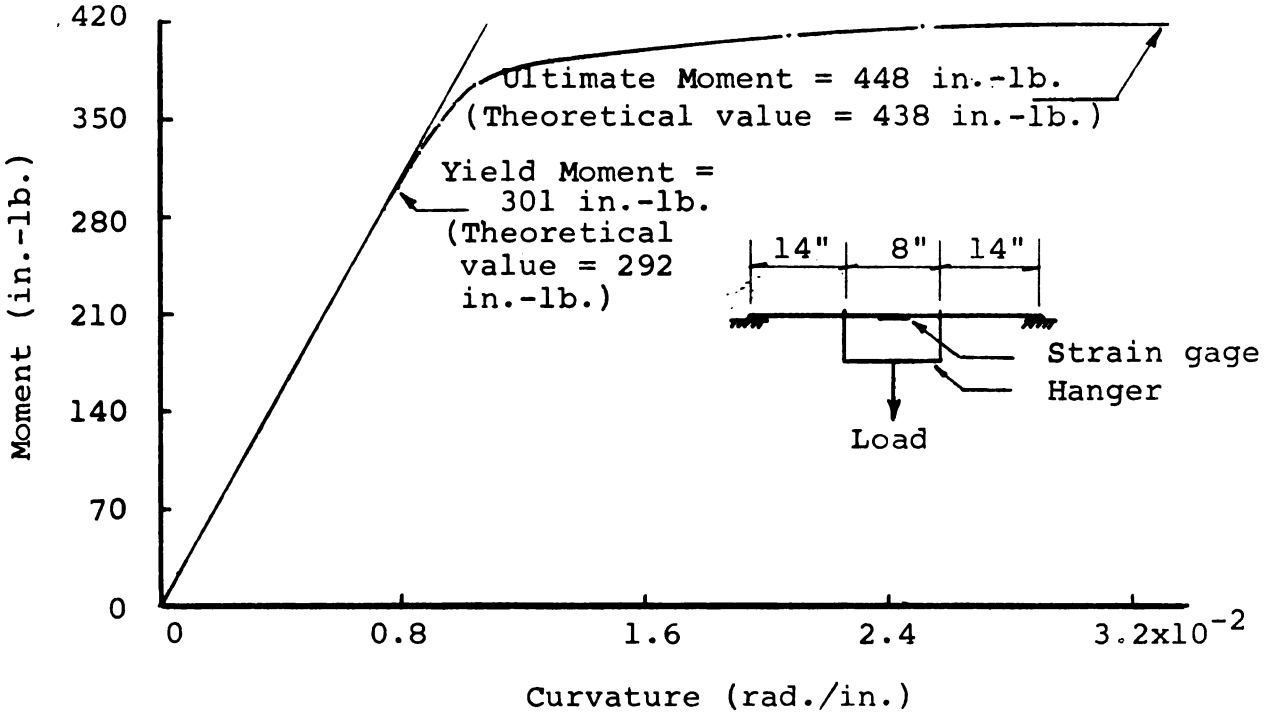

Figure 7-- Moment-curvature diagram.

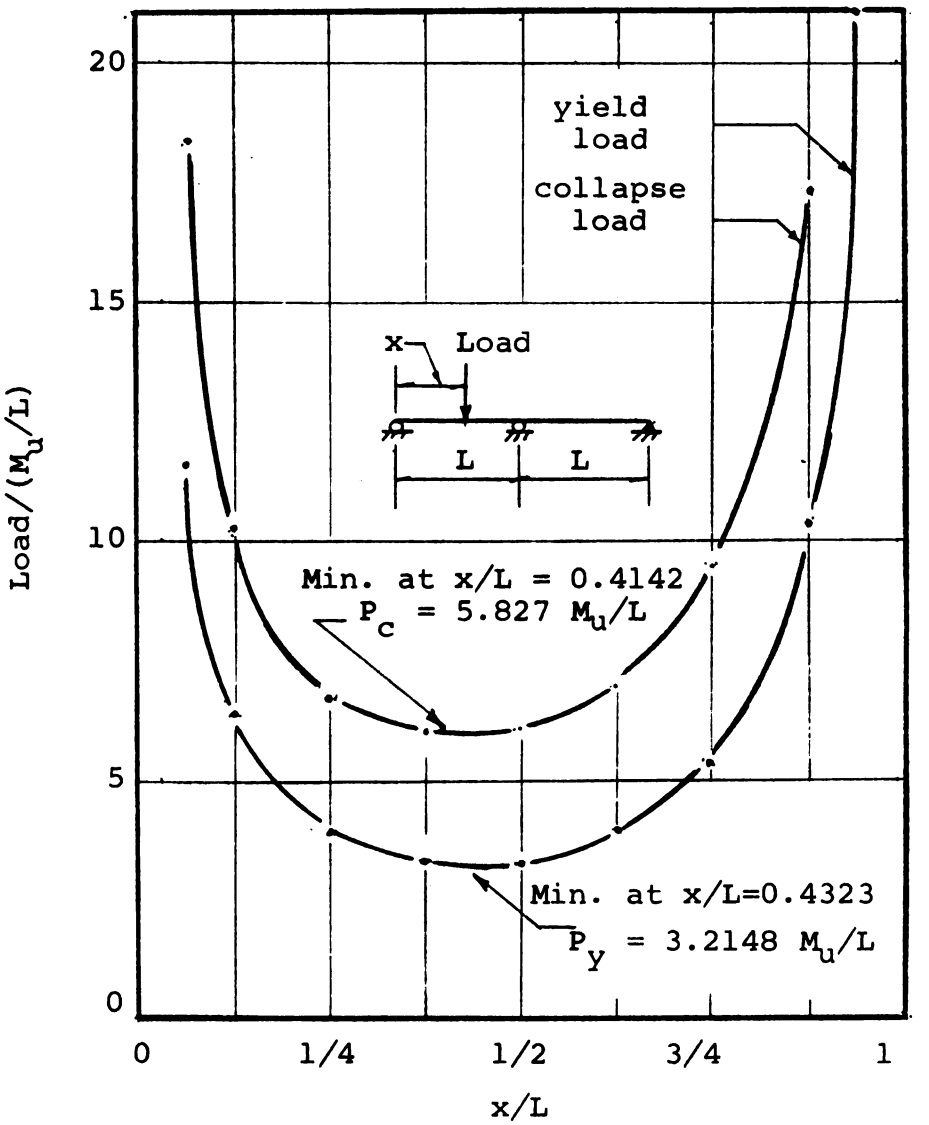

P_y β 1.0

$P_c = 1.8125\ P_y$ $\beta = 1.8125$

P_y = 38.3709 lb. (for σ_y=27500 psi)

P_c = 69.5493 lb. (for σ_y=27500 psi)

Figure 8--Curves of yield load and collapse load.

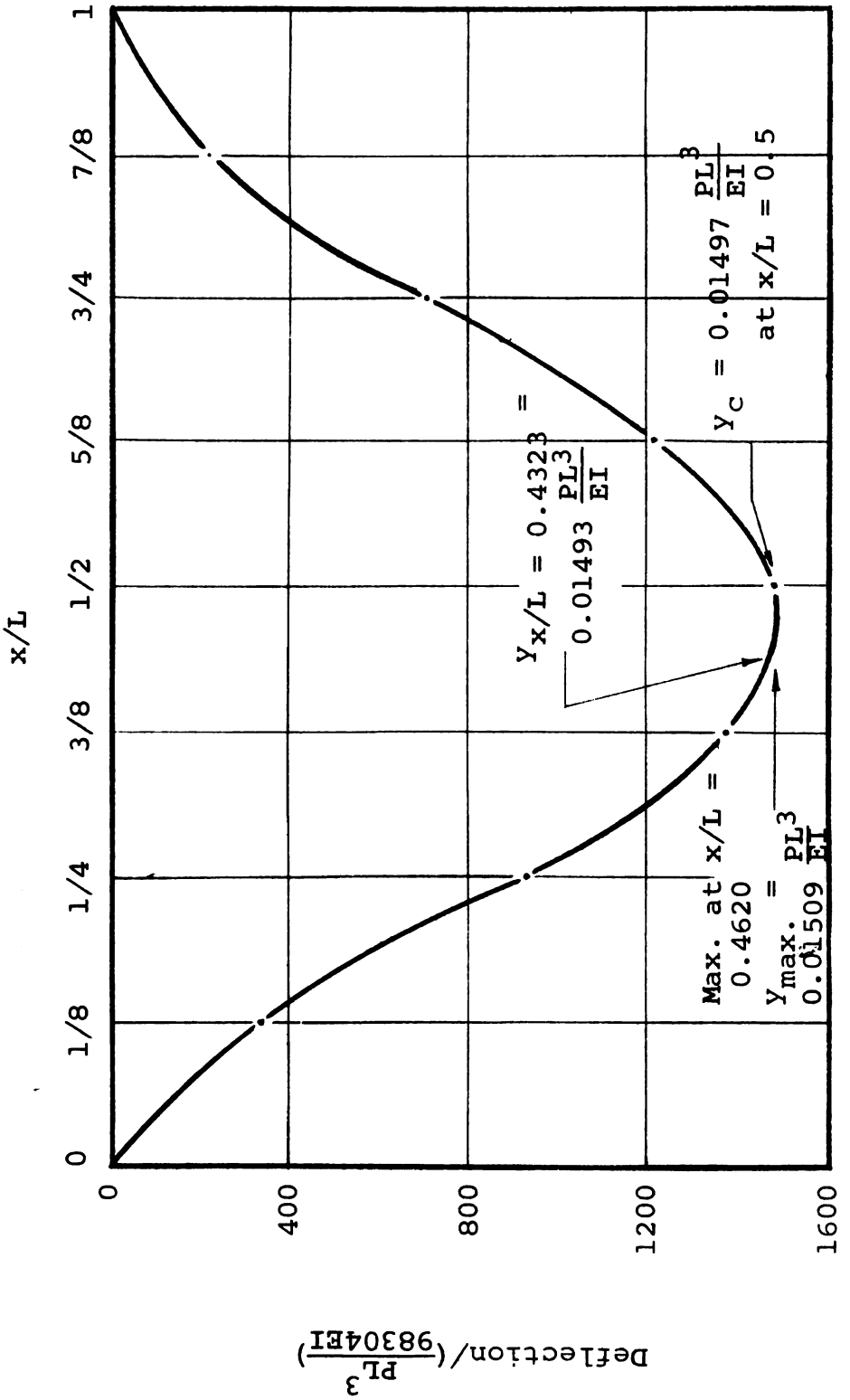

Figure 9 -- Deflection at point of loading.

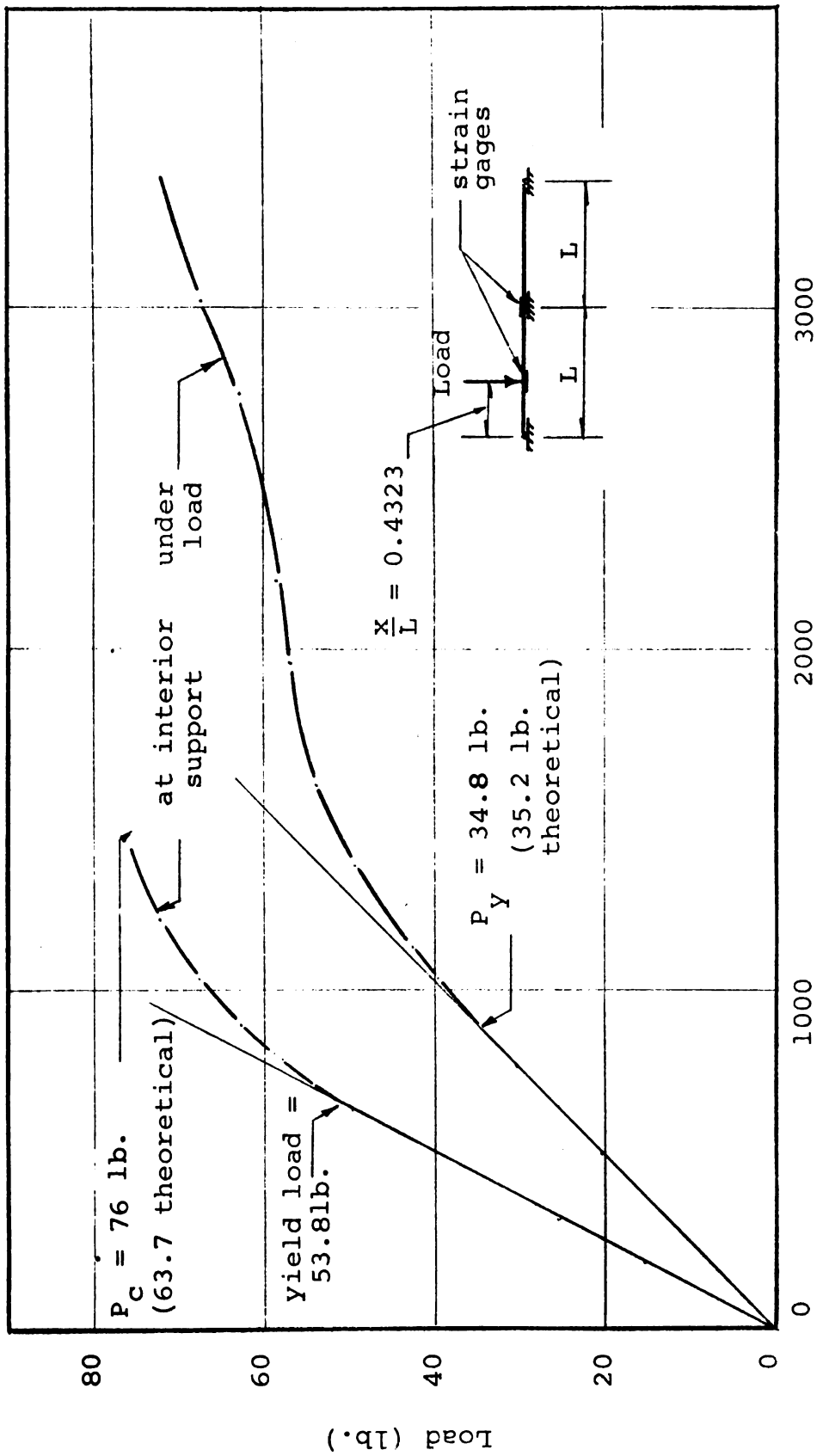

Figure 10--Static behavior of two-span continuous beam.

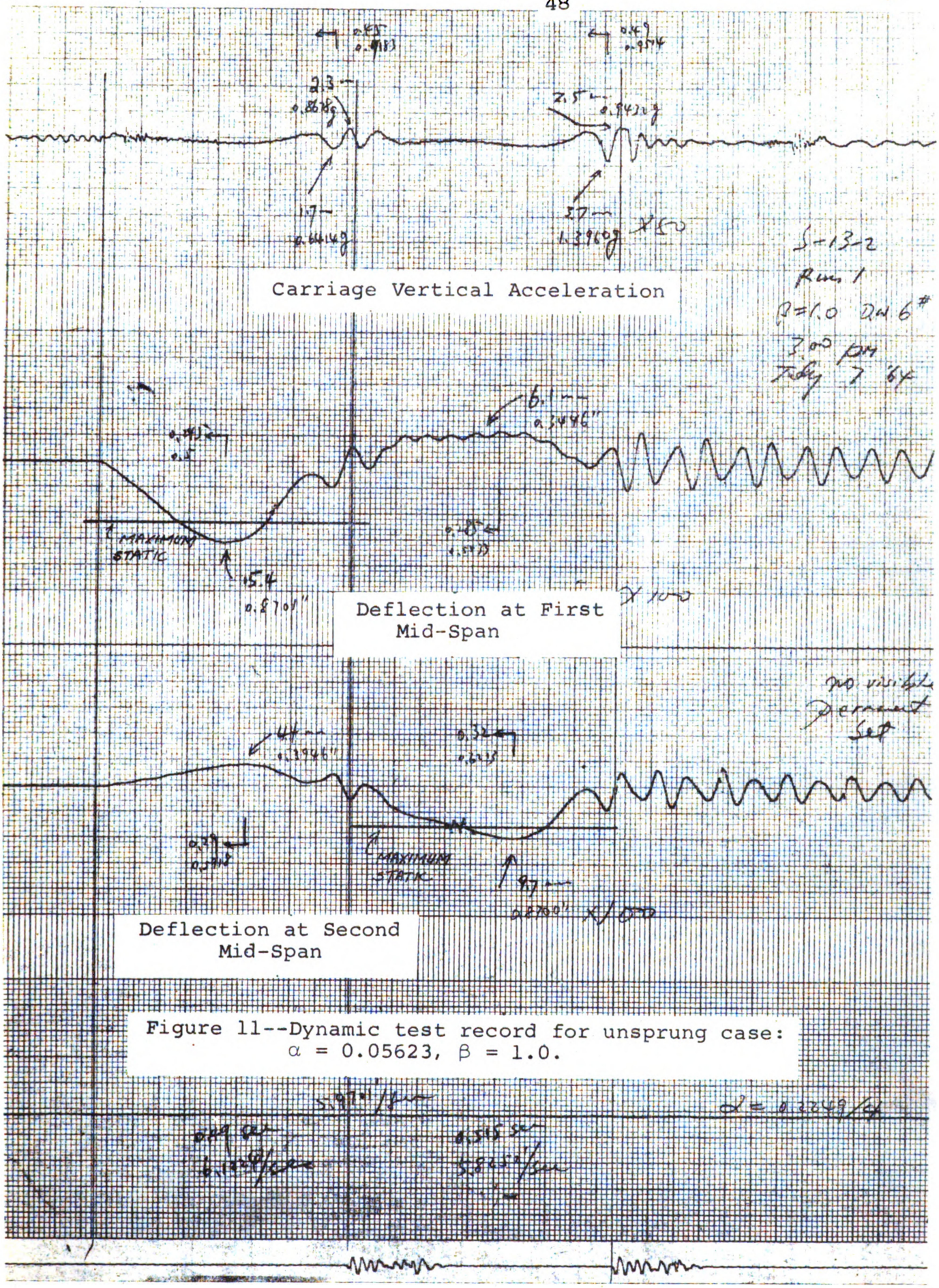

Figure 11--Dynamic test record for unsprung case: $\alpha = 0.05623$, $\beta = 1.0$.

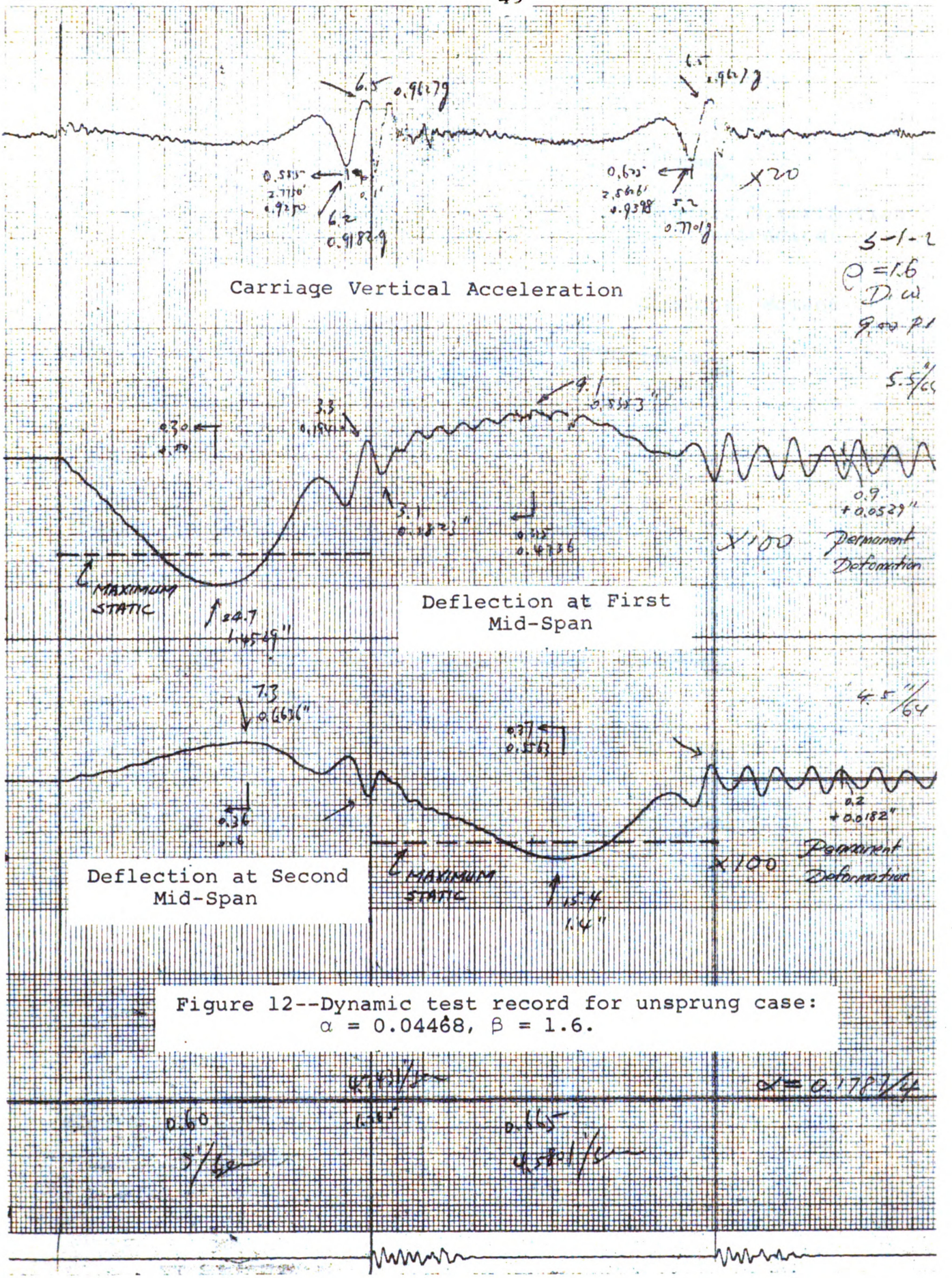

Figure 12--Dynamic test record for unsprung case: $\alpha = 0.04468$, $\beta = 1.6$.

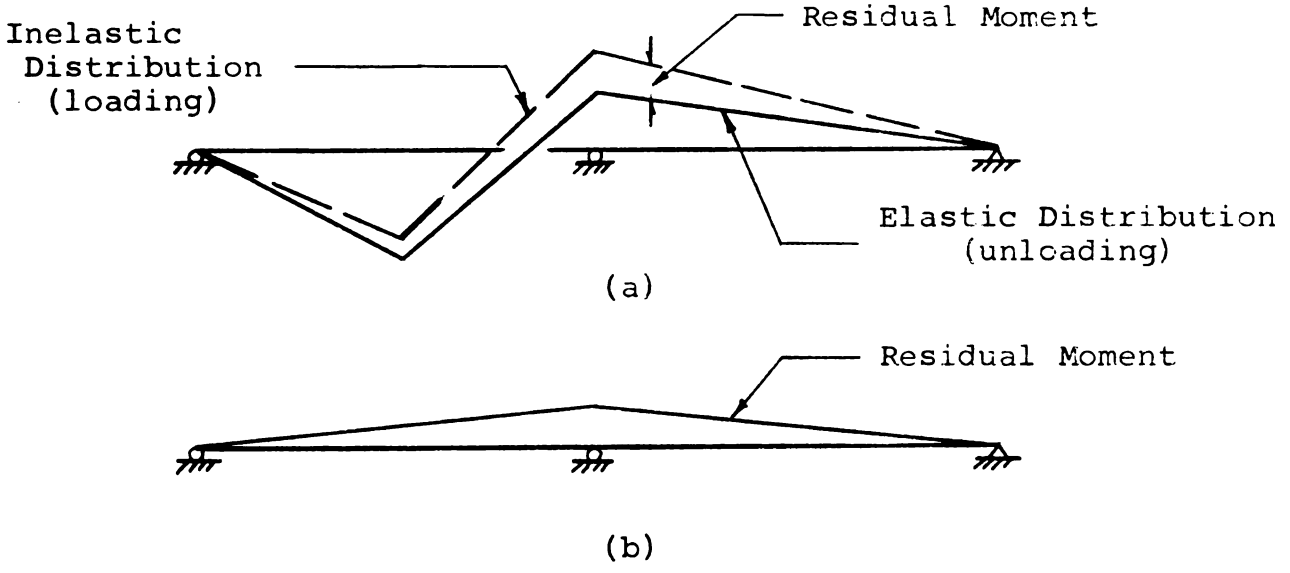

Figure 13 -- Distribution of residual moment.

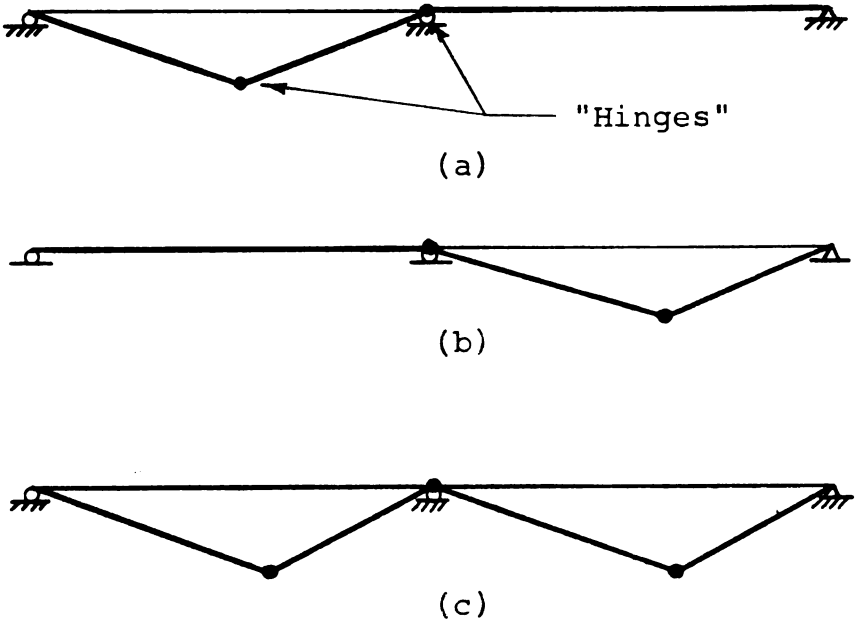

Figure 14--Final deformed shapes.

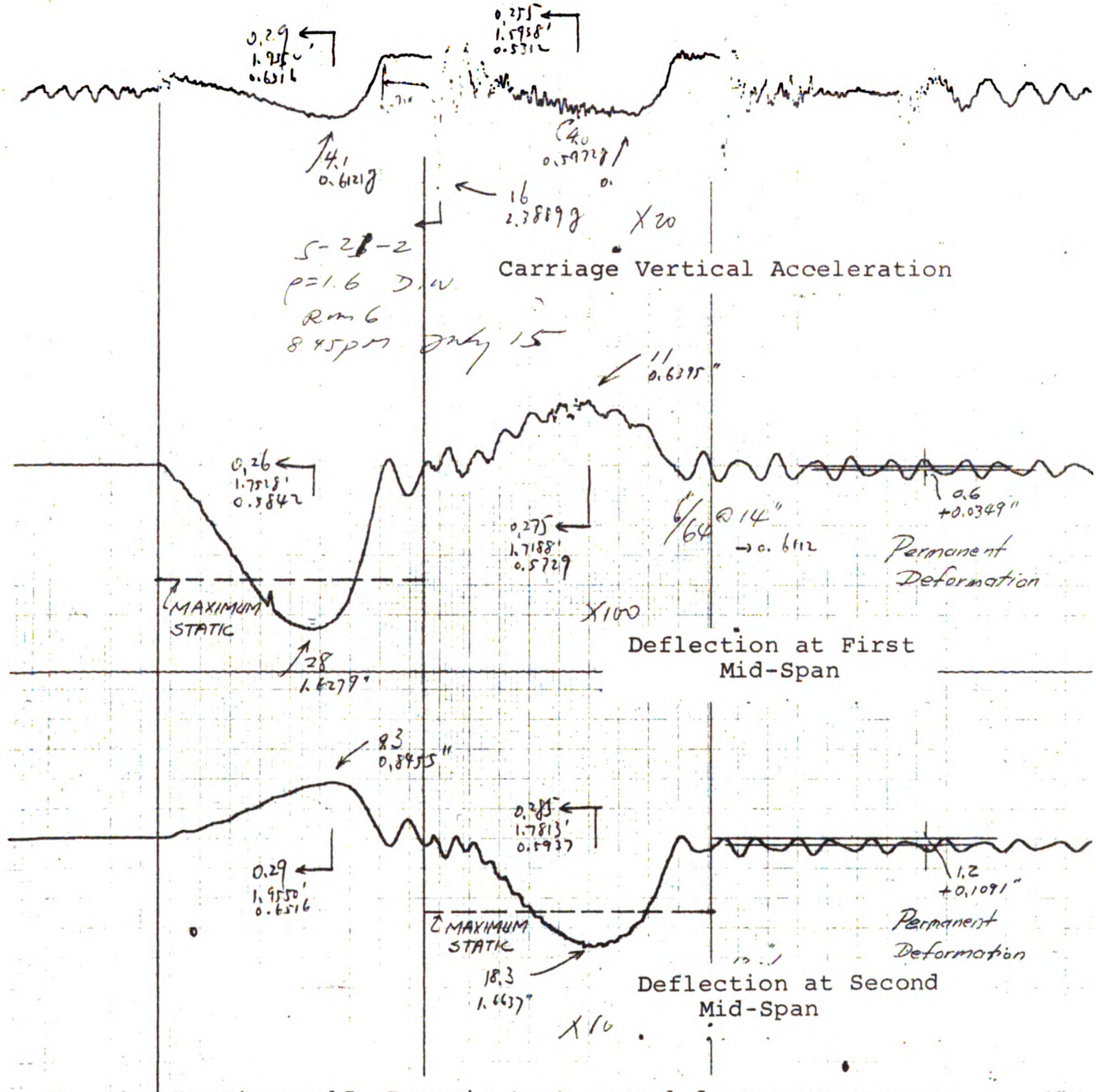

Figure 15--Dynamic test record for unsprung case: $\alpha = 0.06108$, β 1.6.

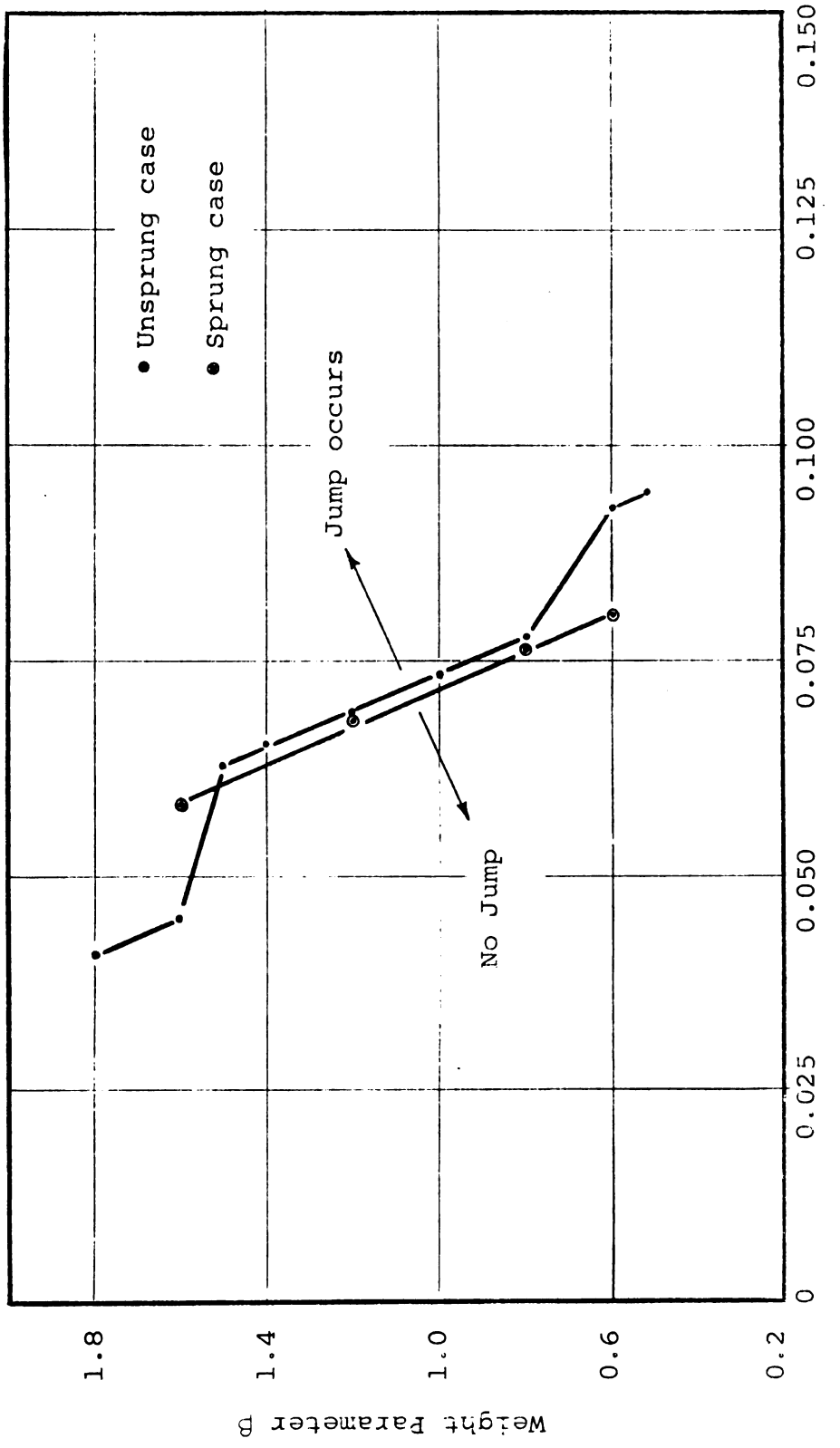

Figure 16--"Jump lines."

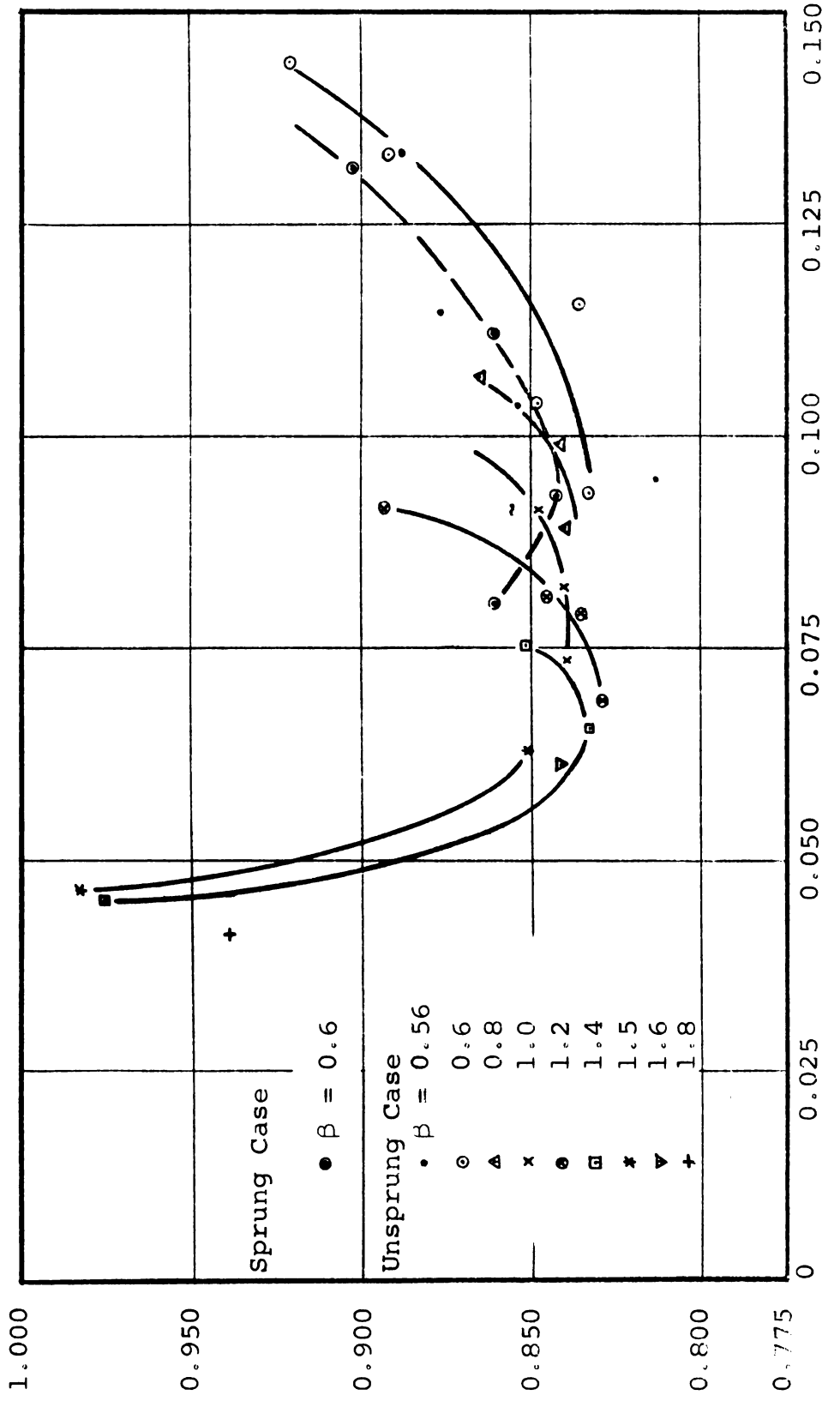

Figure 17 -- Location of starting position of jump.

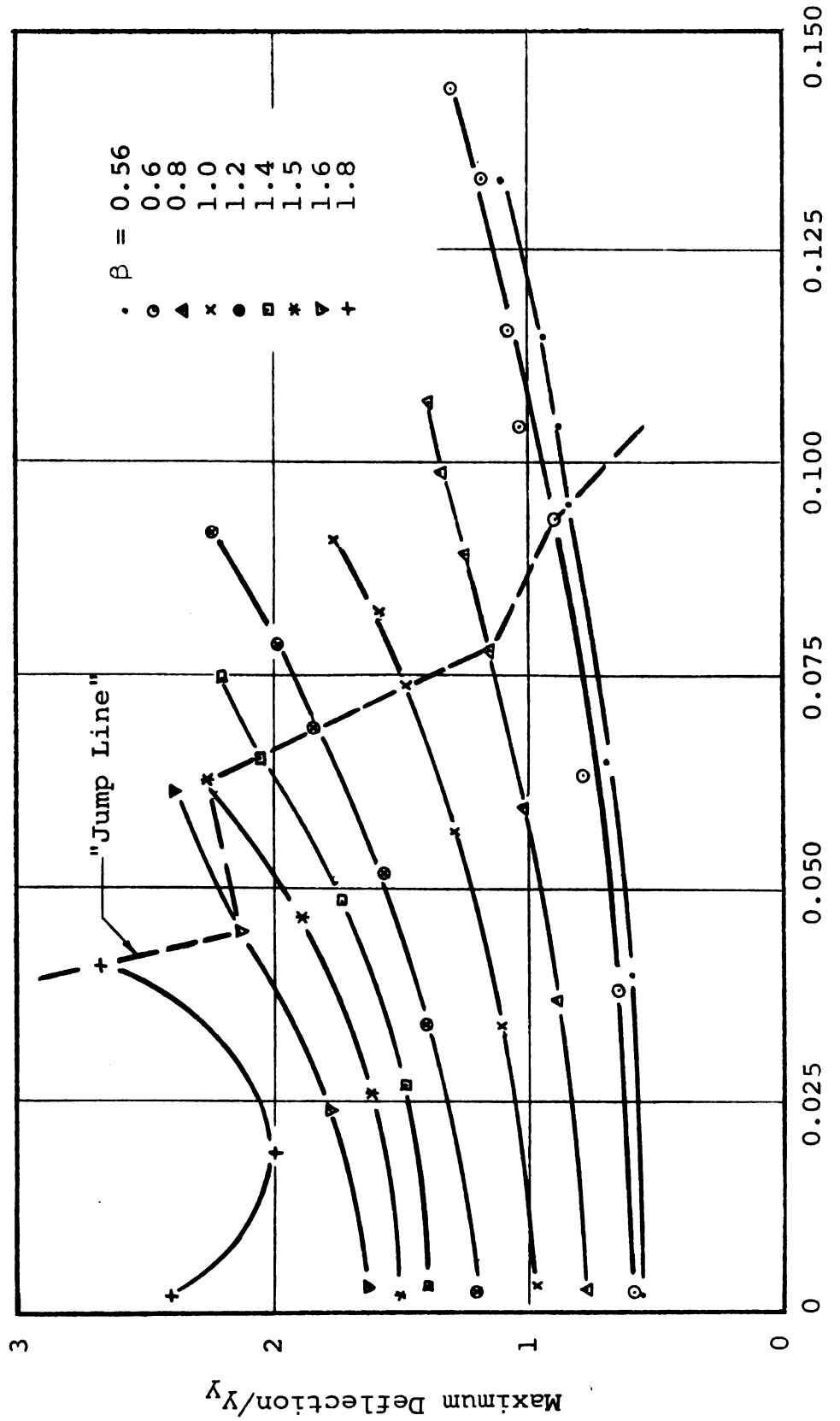

Figure 18--Maximum deflection of first mid-span (unsprung case).

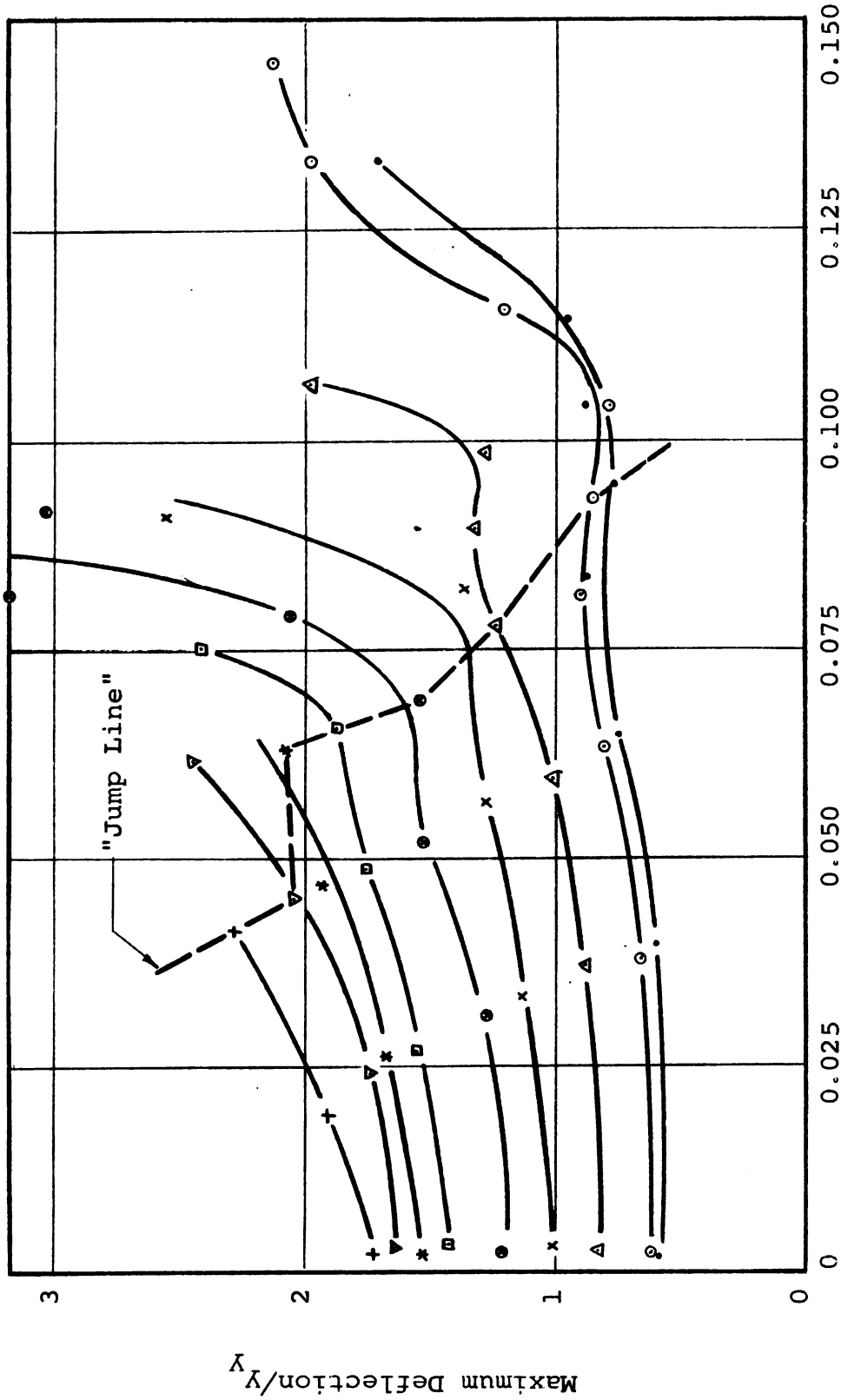

Figure 19--Maximum deflection of second mid-span (unsprung case).

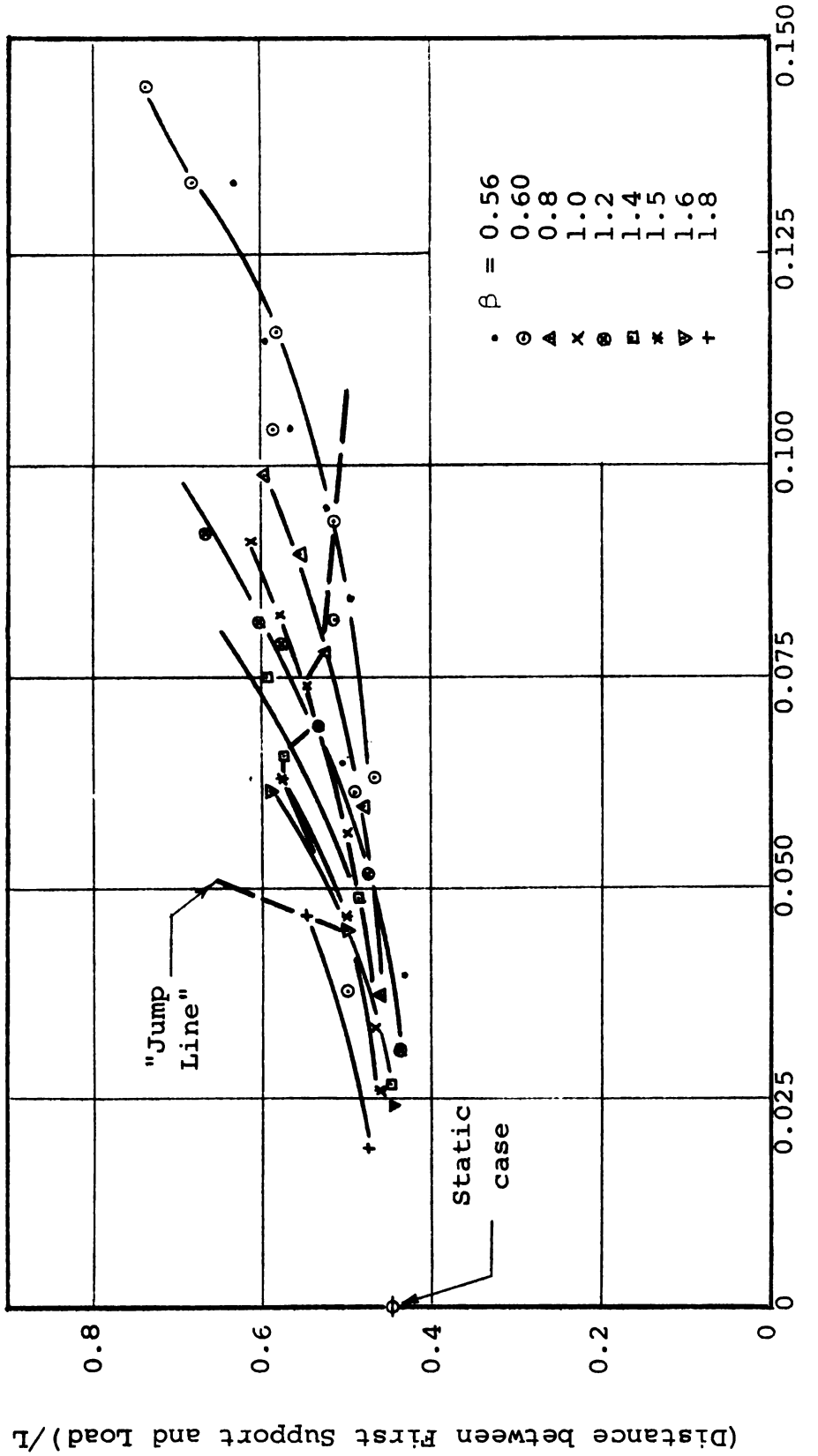

Figure 20--Location of load for maximum deflection of first mid-span (unsprung case).

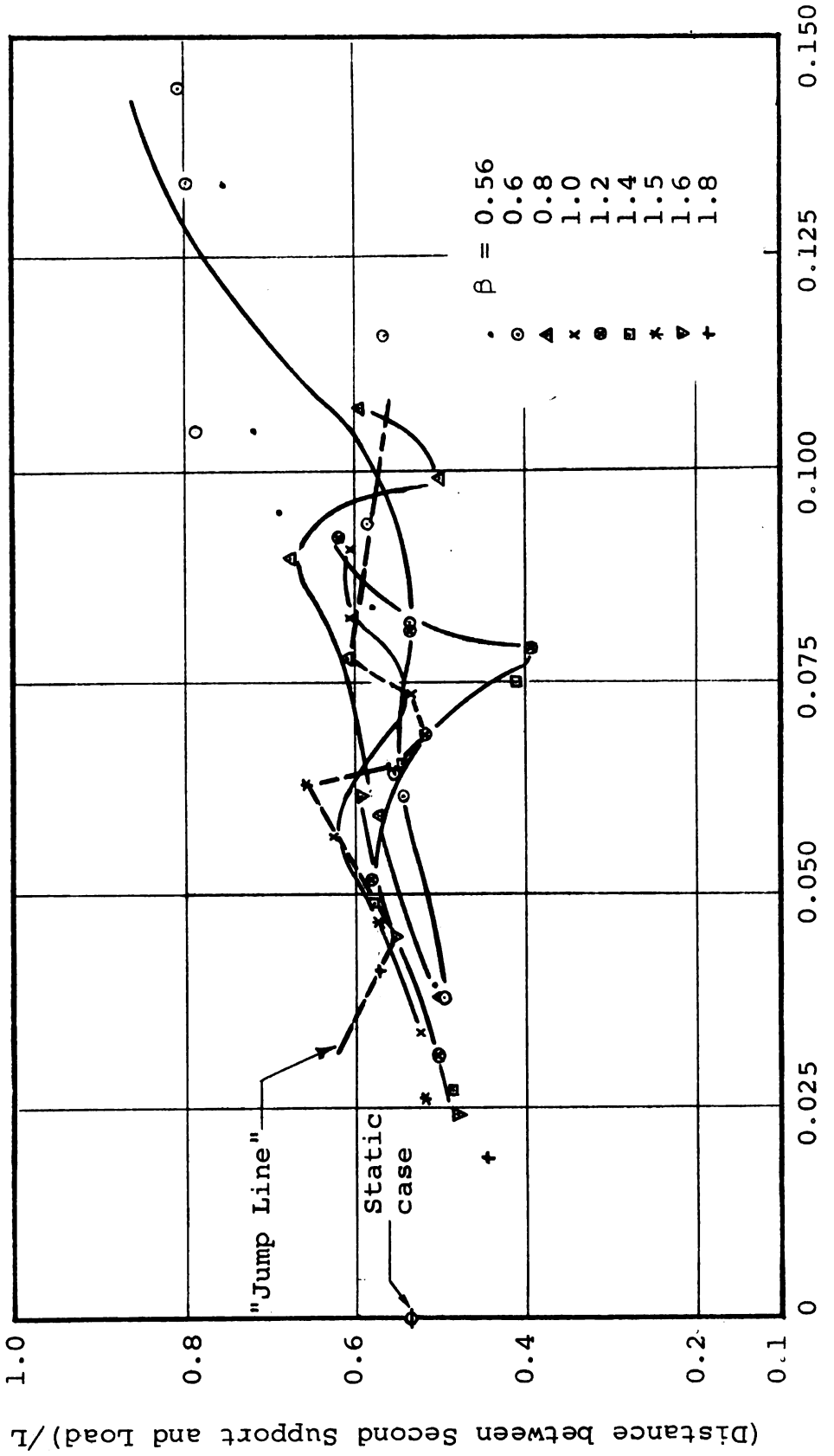

Figure 21--Location of load for maximum deflection of second mid-span (unsprung case).

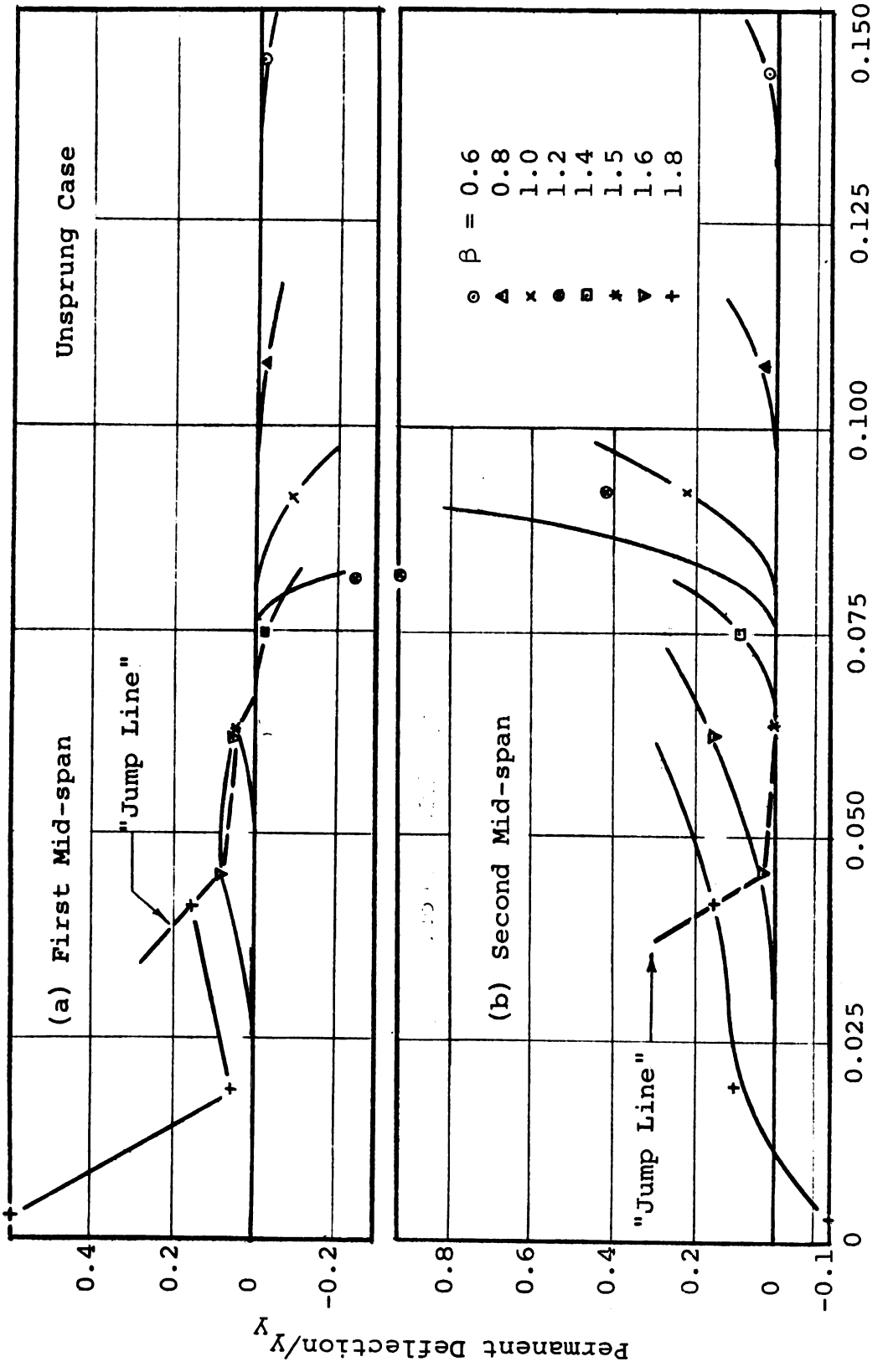

Figure 22--Permanent deflections.

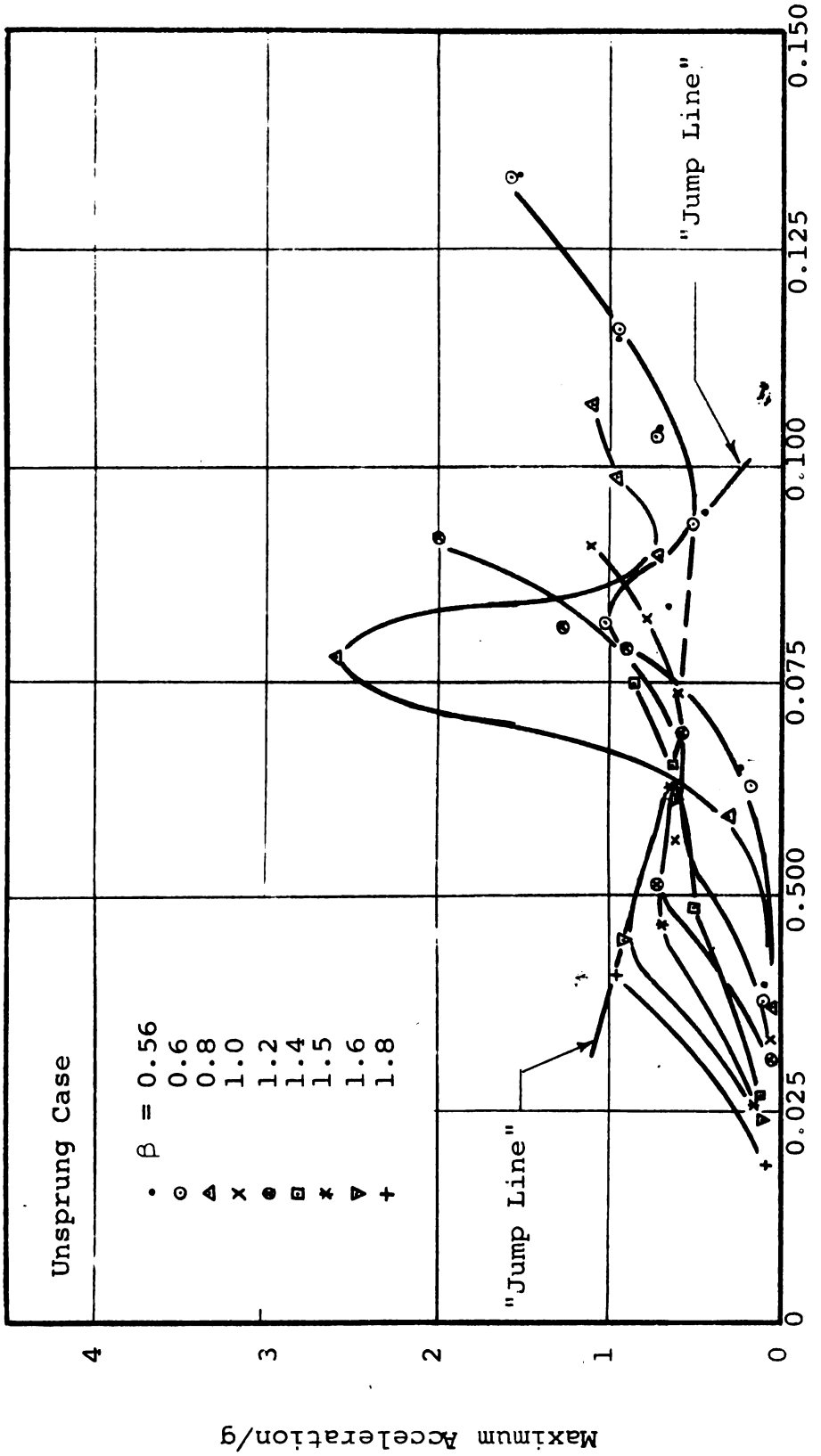

Figure 23--Maximum vertical acceleration of load on first span.

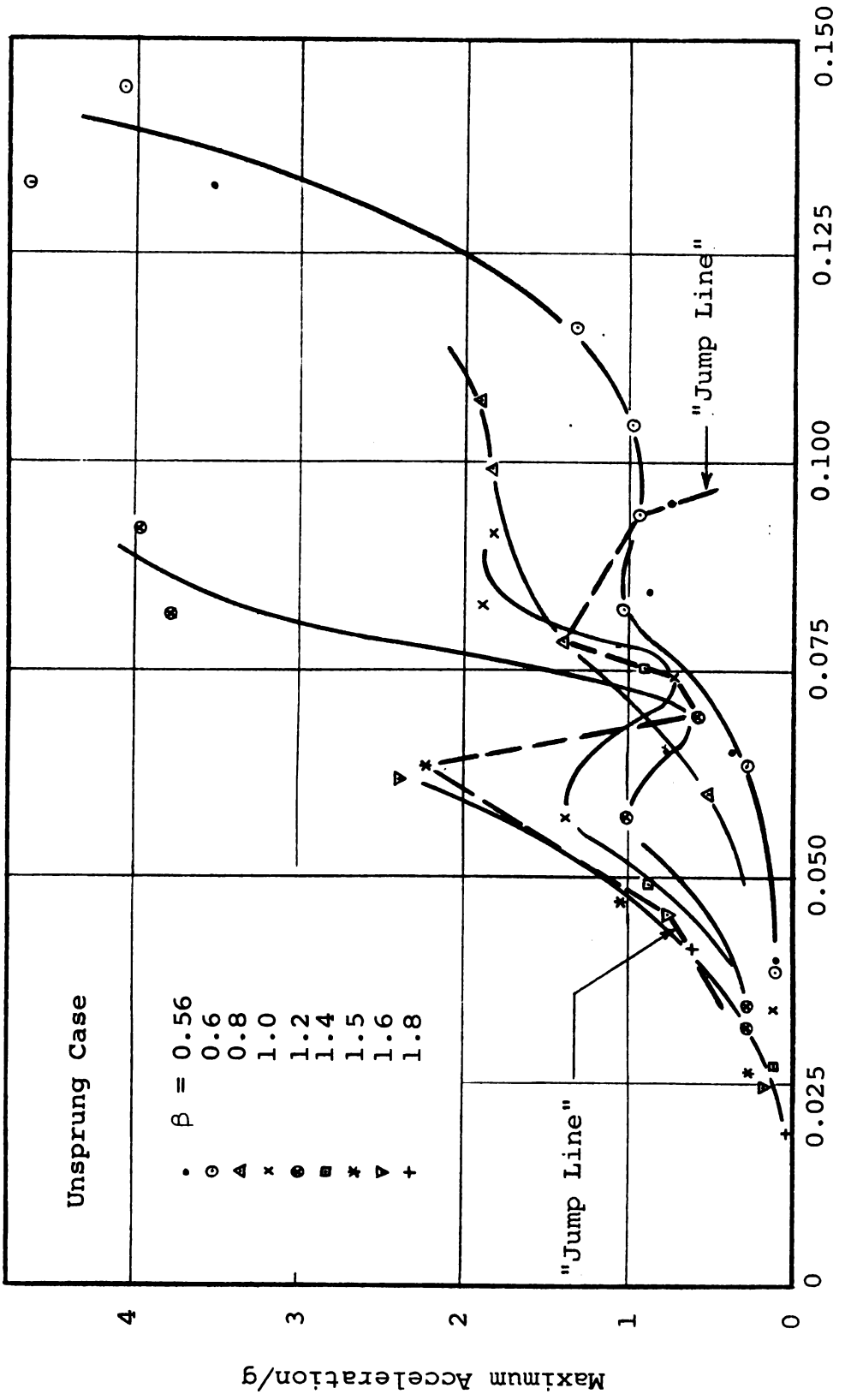

Figure 24--Maximum vertical acceleration of load on second span.

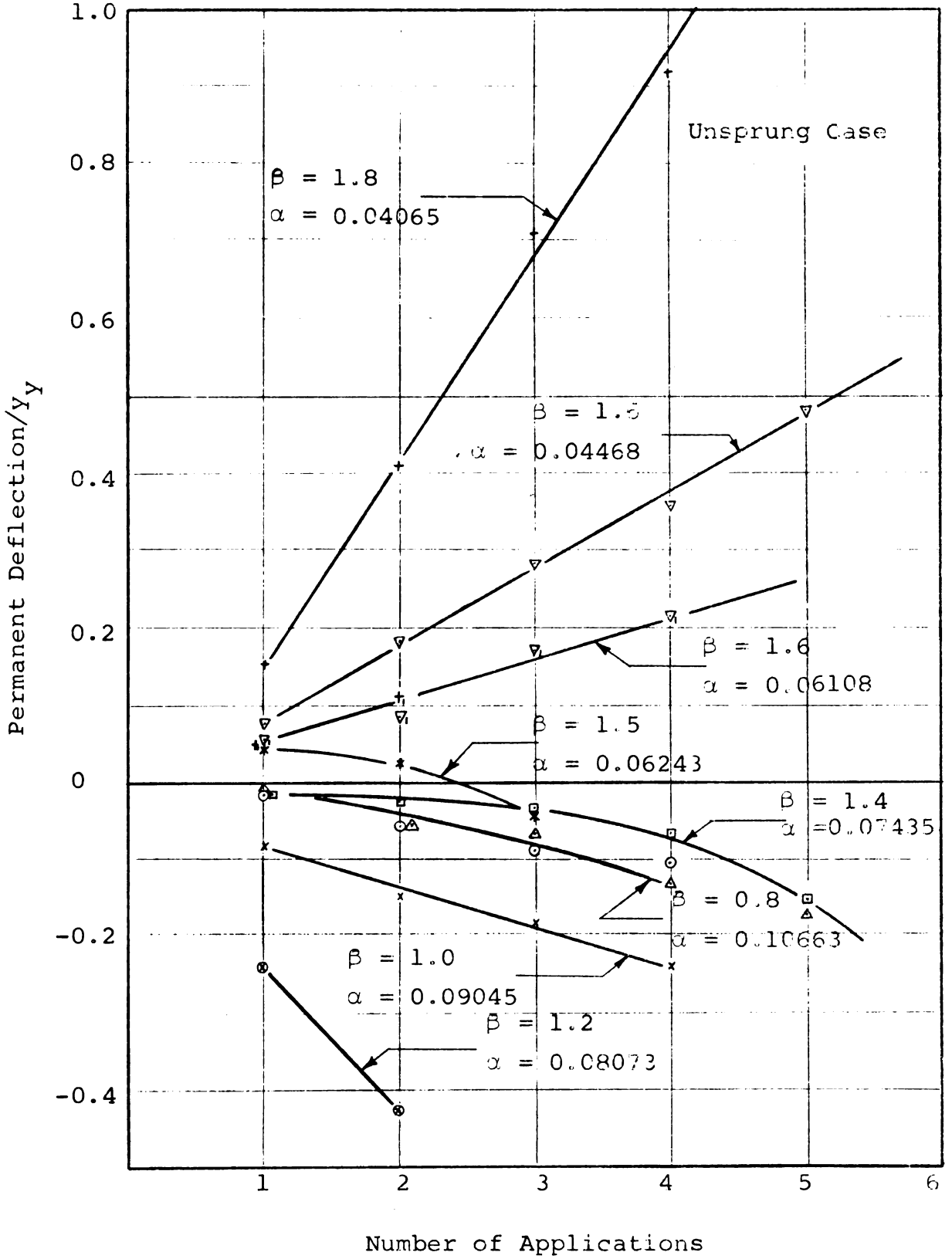

Figure 25--Permanent deflection of first mid-span under repeated loading.

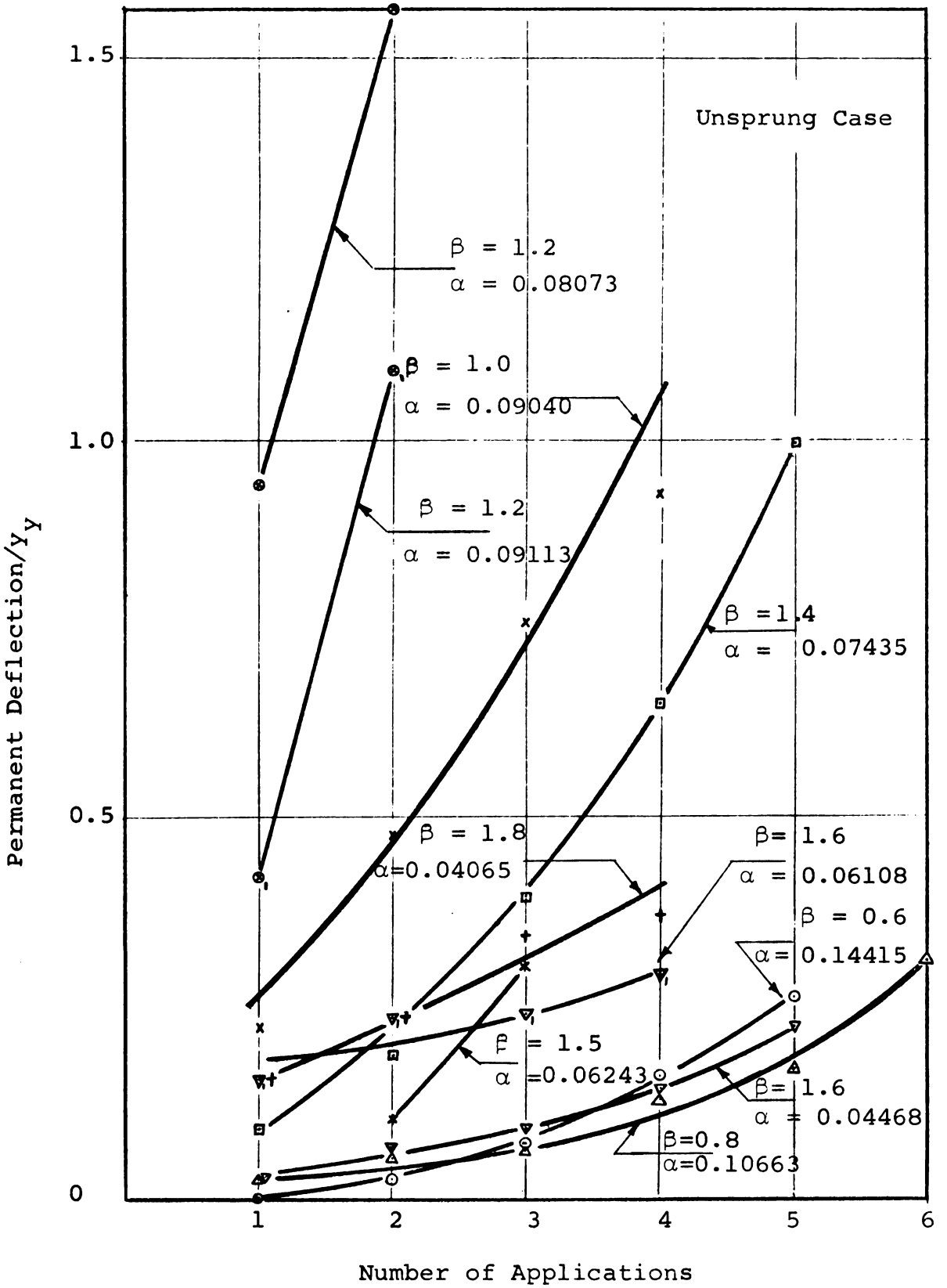

Figure 26. Permanent deflection of second mid-span under repeated loading.

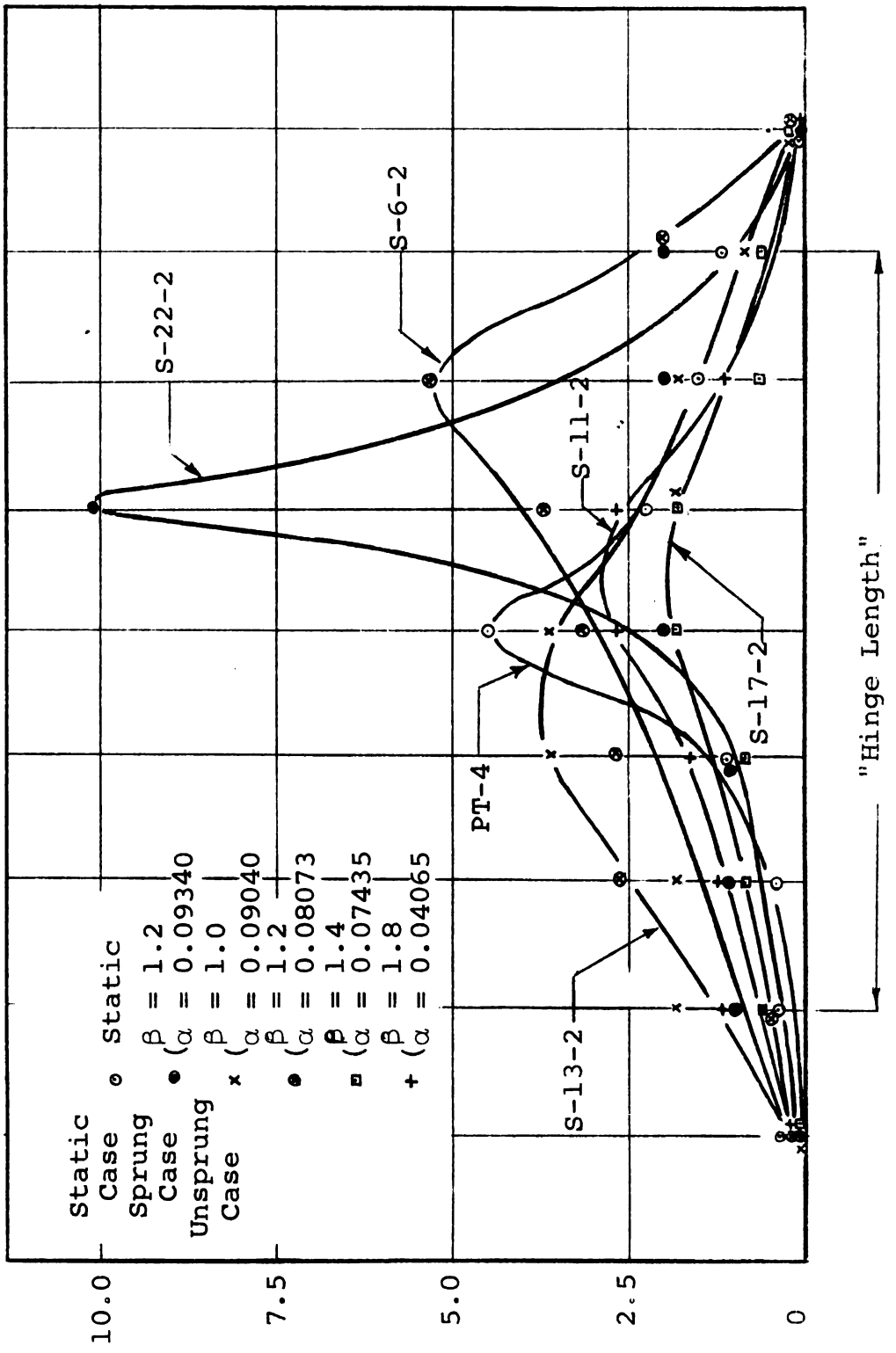

Figure 27--Variation of permanent curvature within "hinge length."

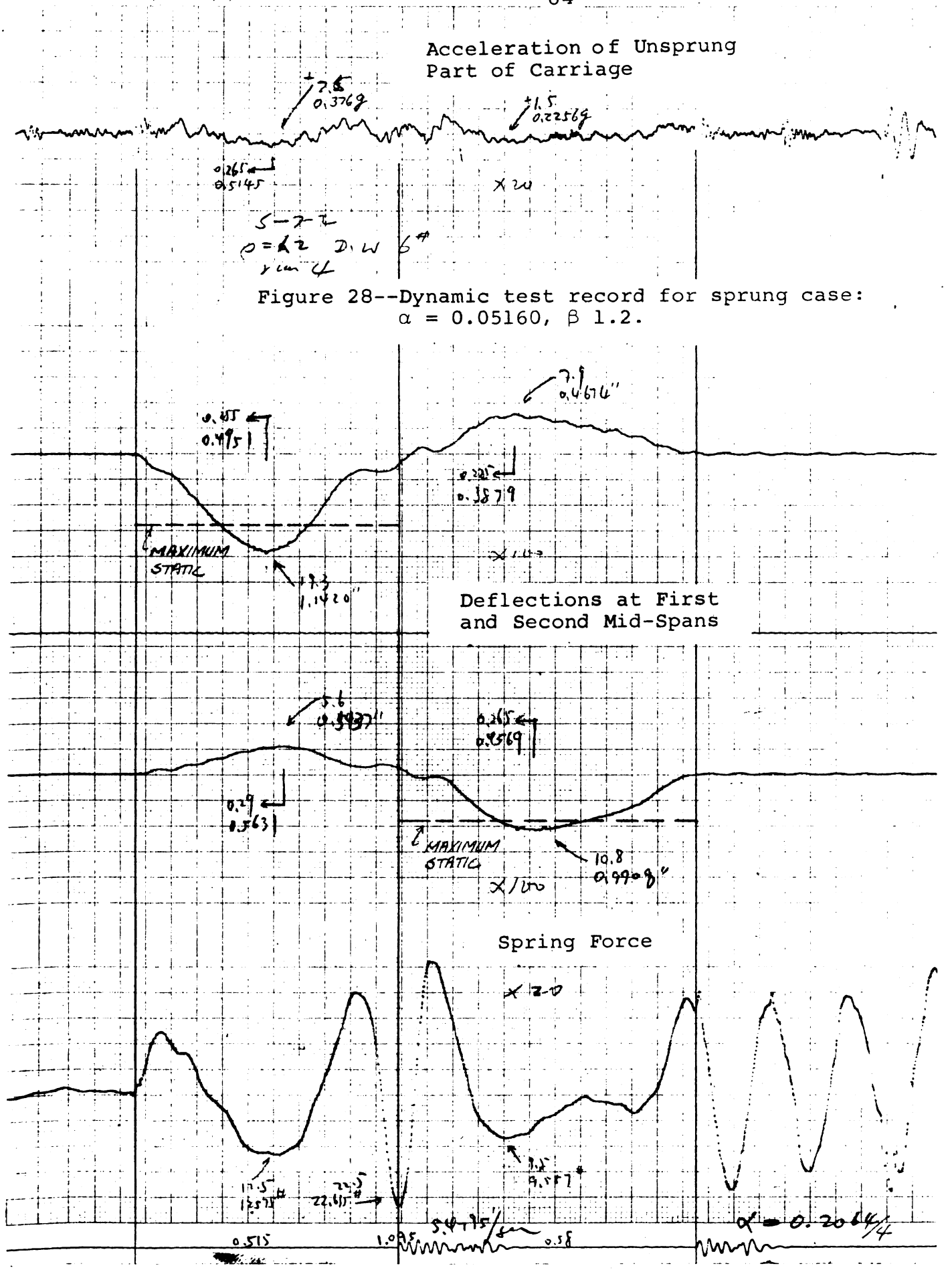

Figure 28--Dynamic test record for sprung case: α = 0.05160, β 1.2.

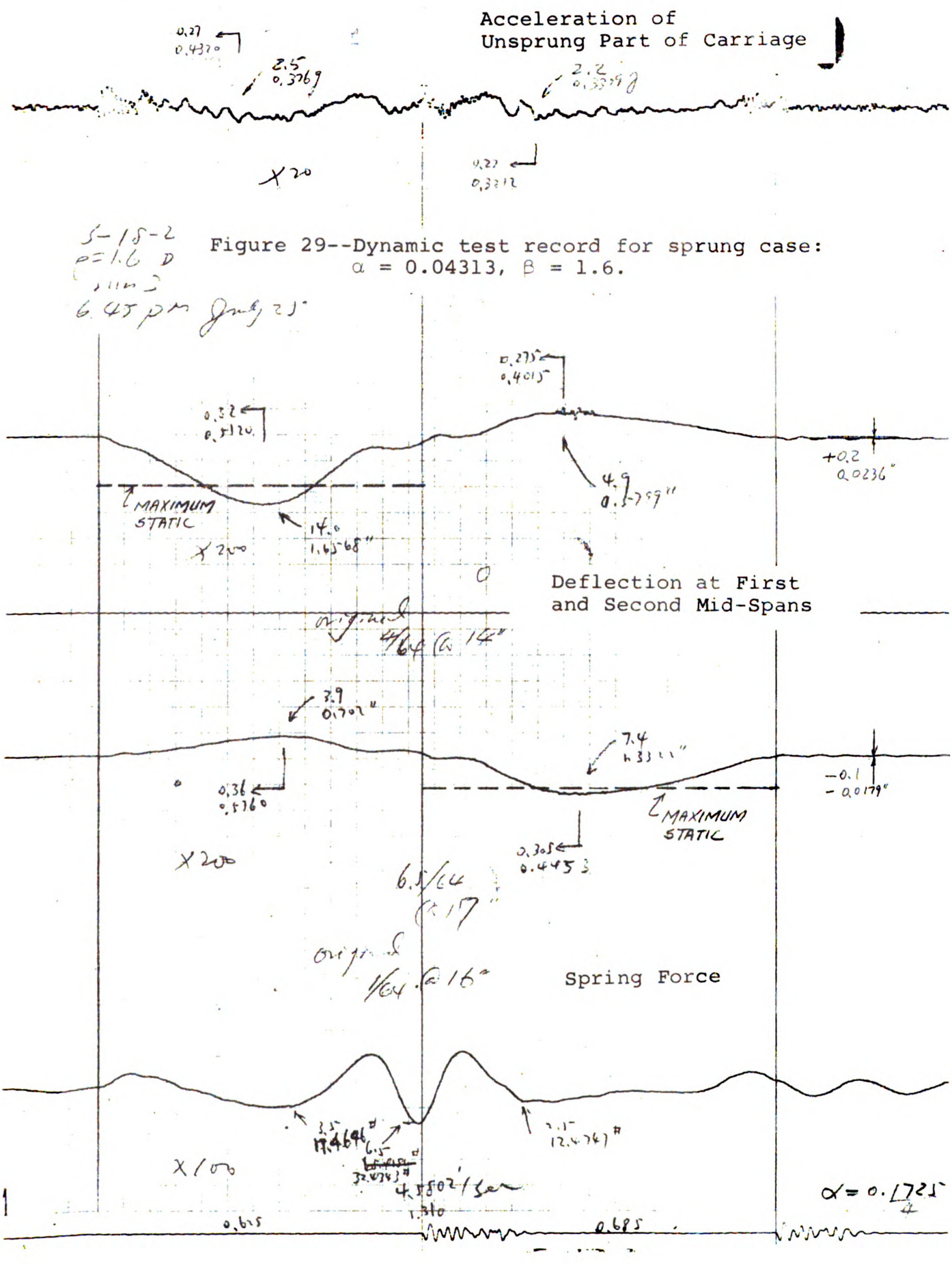

Figure 29--Dynamic test record for sprung case:
$\alpha = 0.04313$, $\beta = 1.6$.

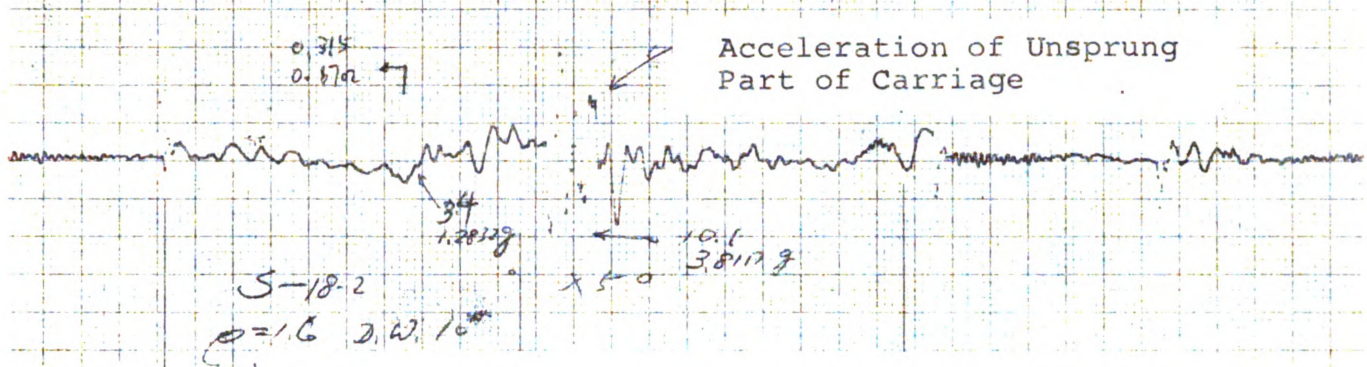

Figure 30--Dynamic test record for sprung case:
$\alpha = 0.05795$, $\beta = 1.6$.

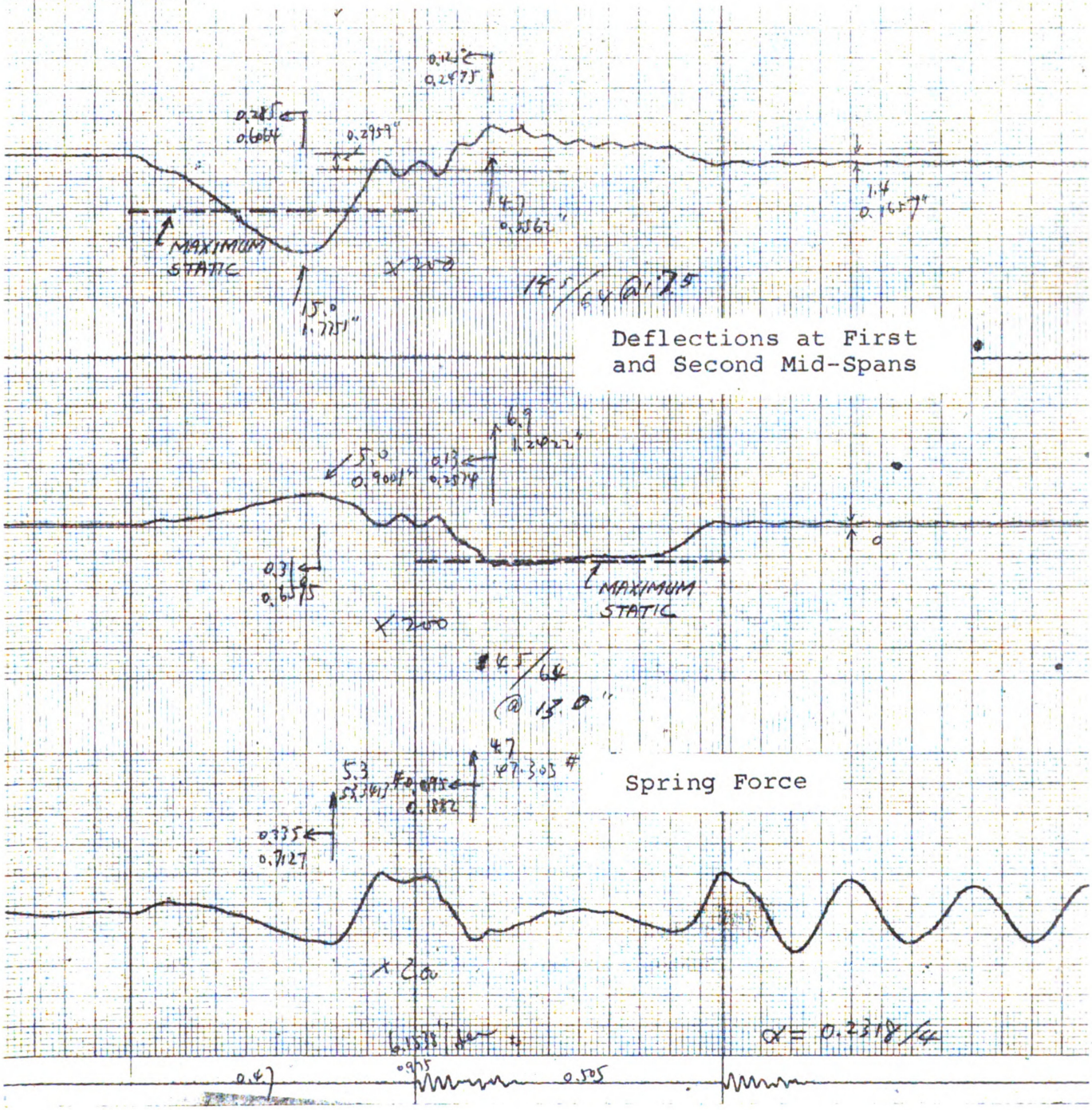

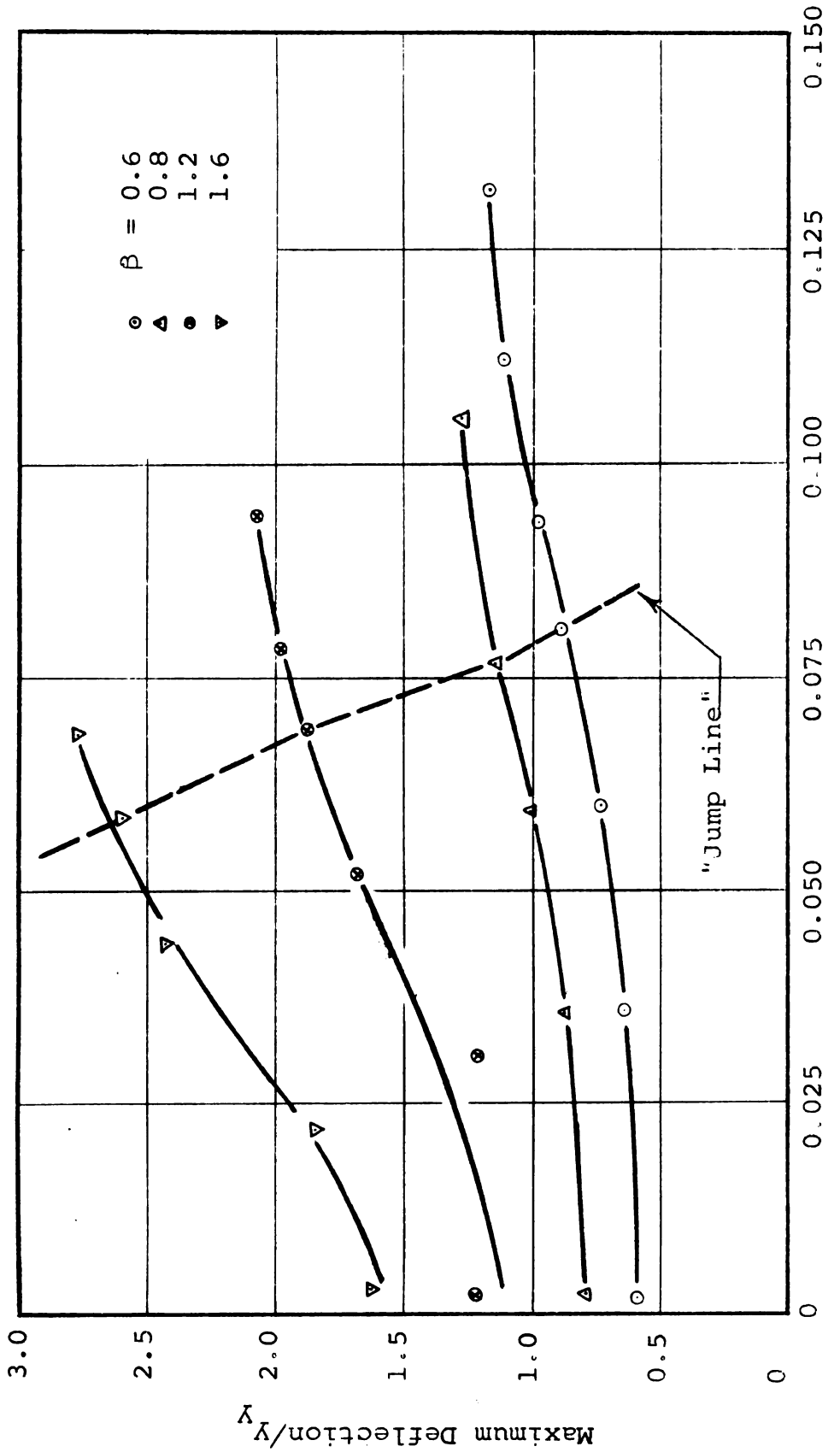

Figure 31--Maximum deflection of first mid-span (sprung case).

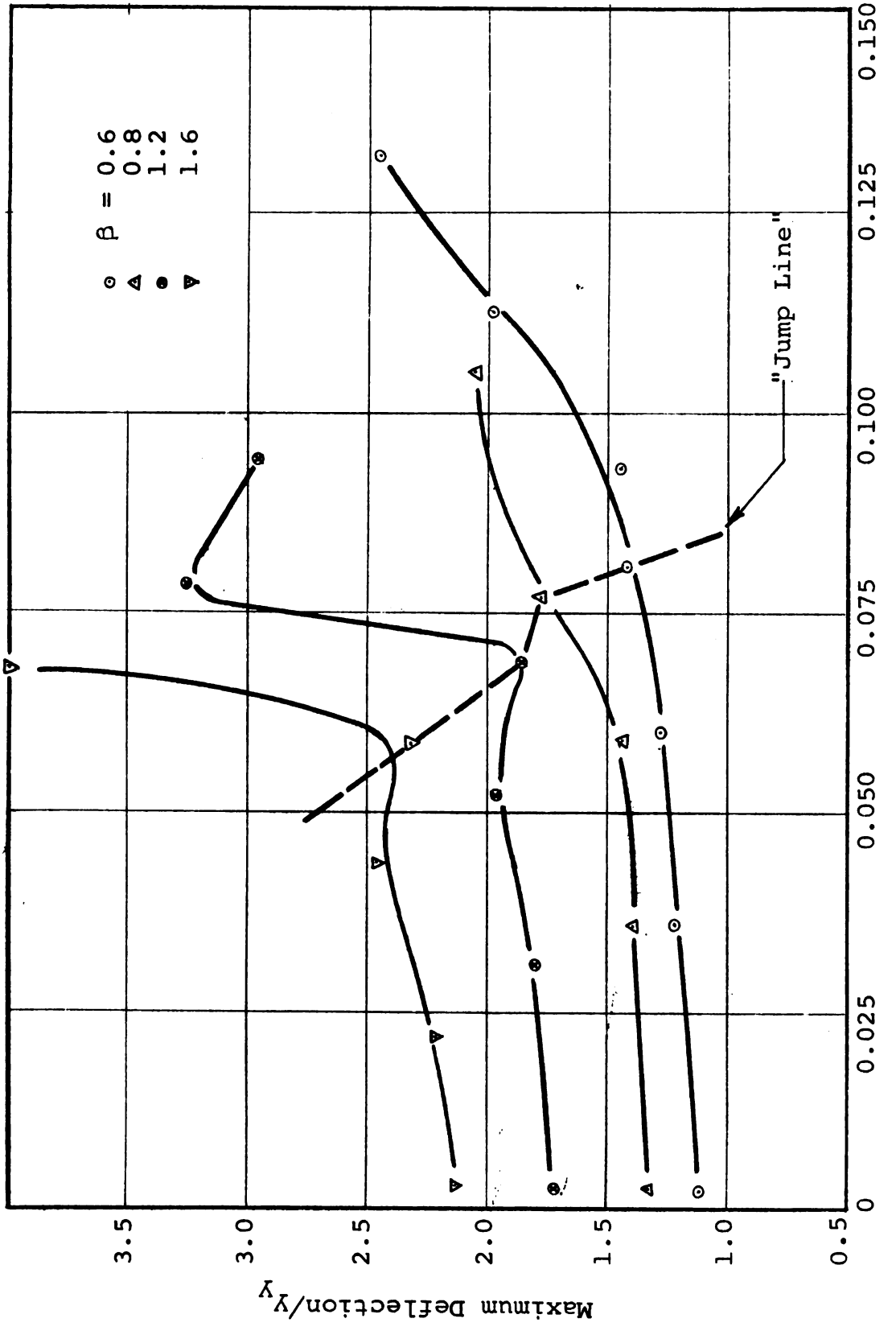

Figure 32. Maximum deflection of second mid-span (sprung case).

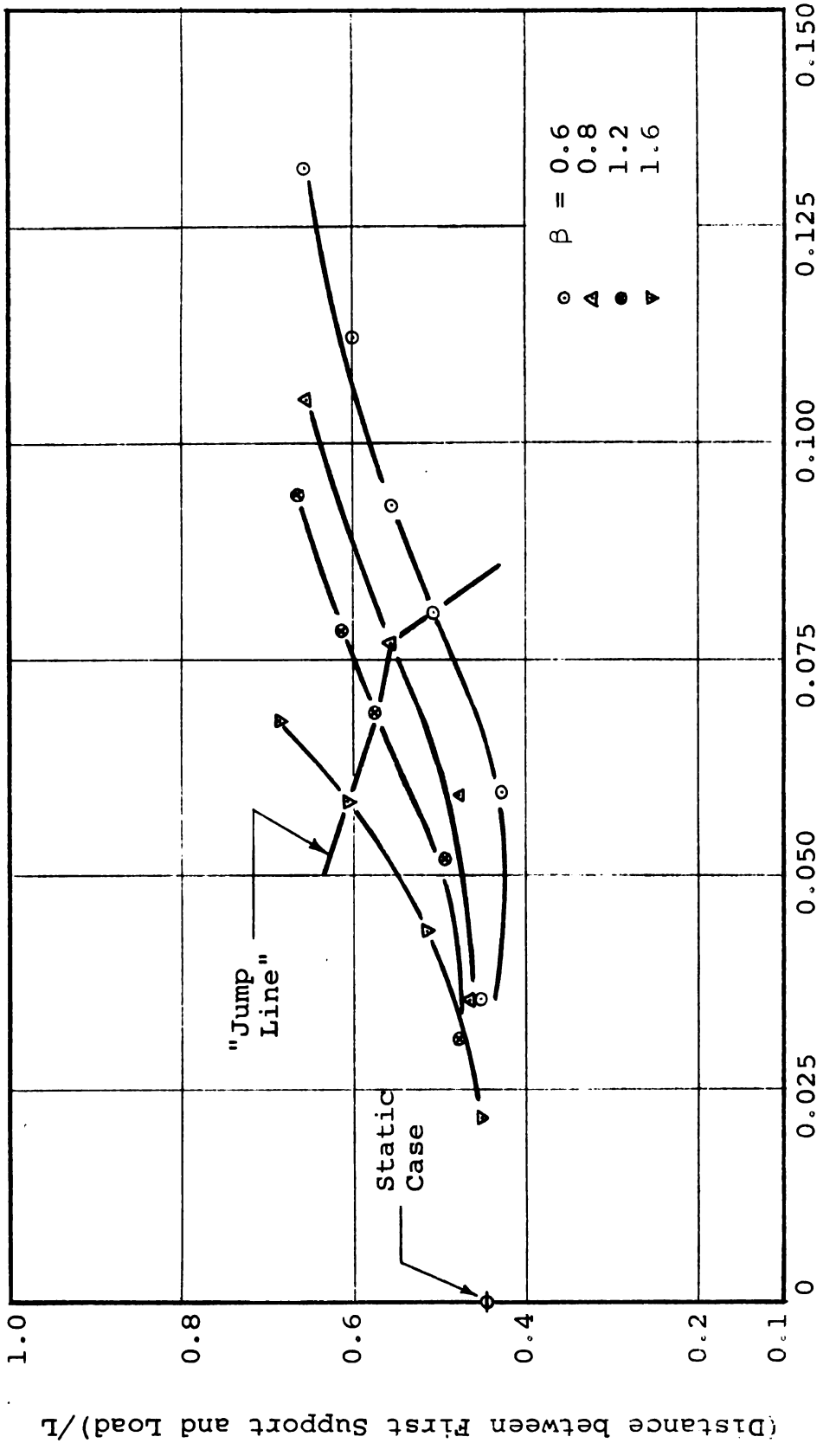

Figure 33--Location of load for maximum deflection of first mid-span (sprung case).

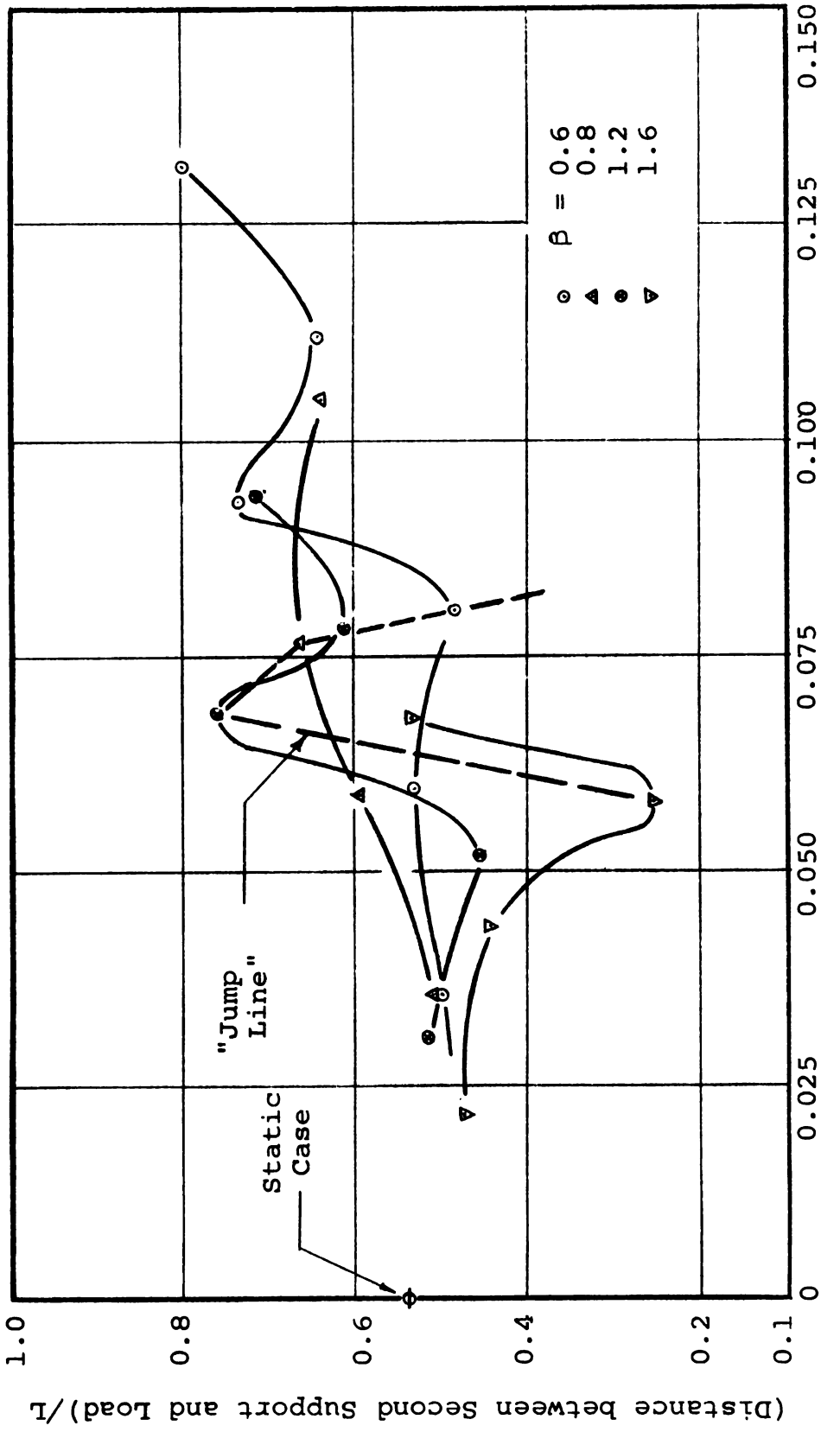

Figure 34--Location of load for maximum deflection of second mid-span (sprung case).

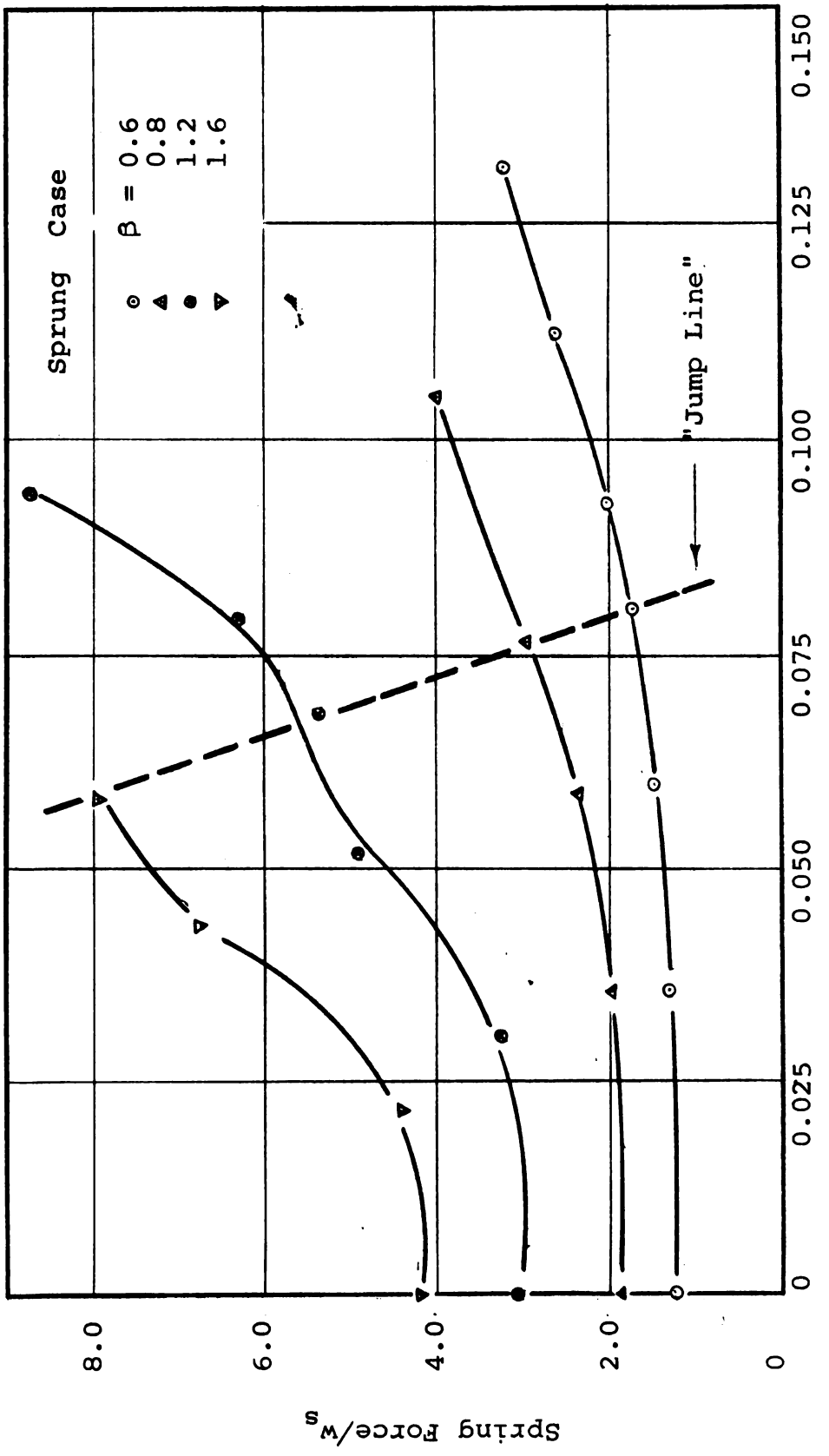

Figure 35--Maximum compressive spring force on first span.

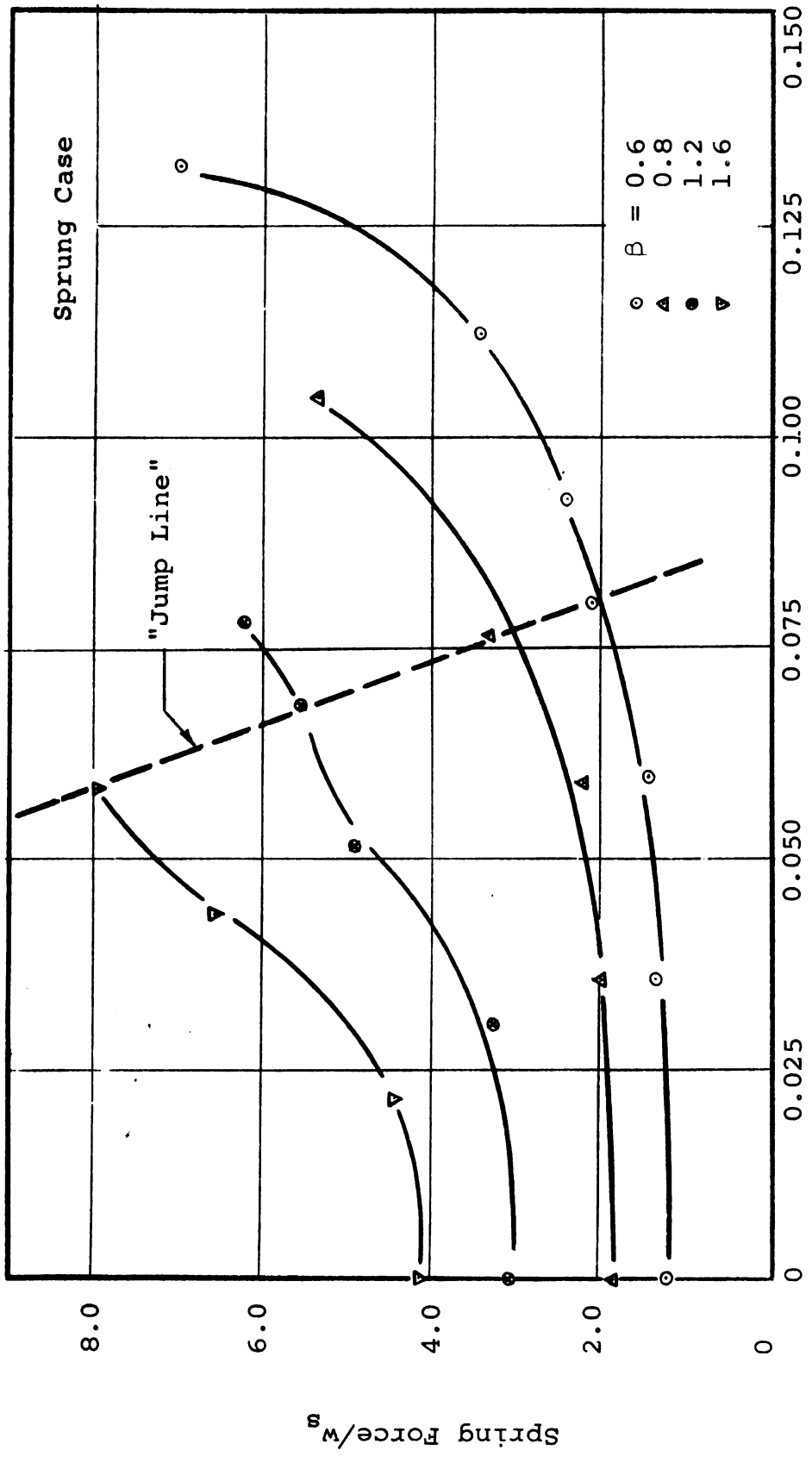

Figure 36--Maximum compressive spring force on second span.

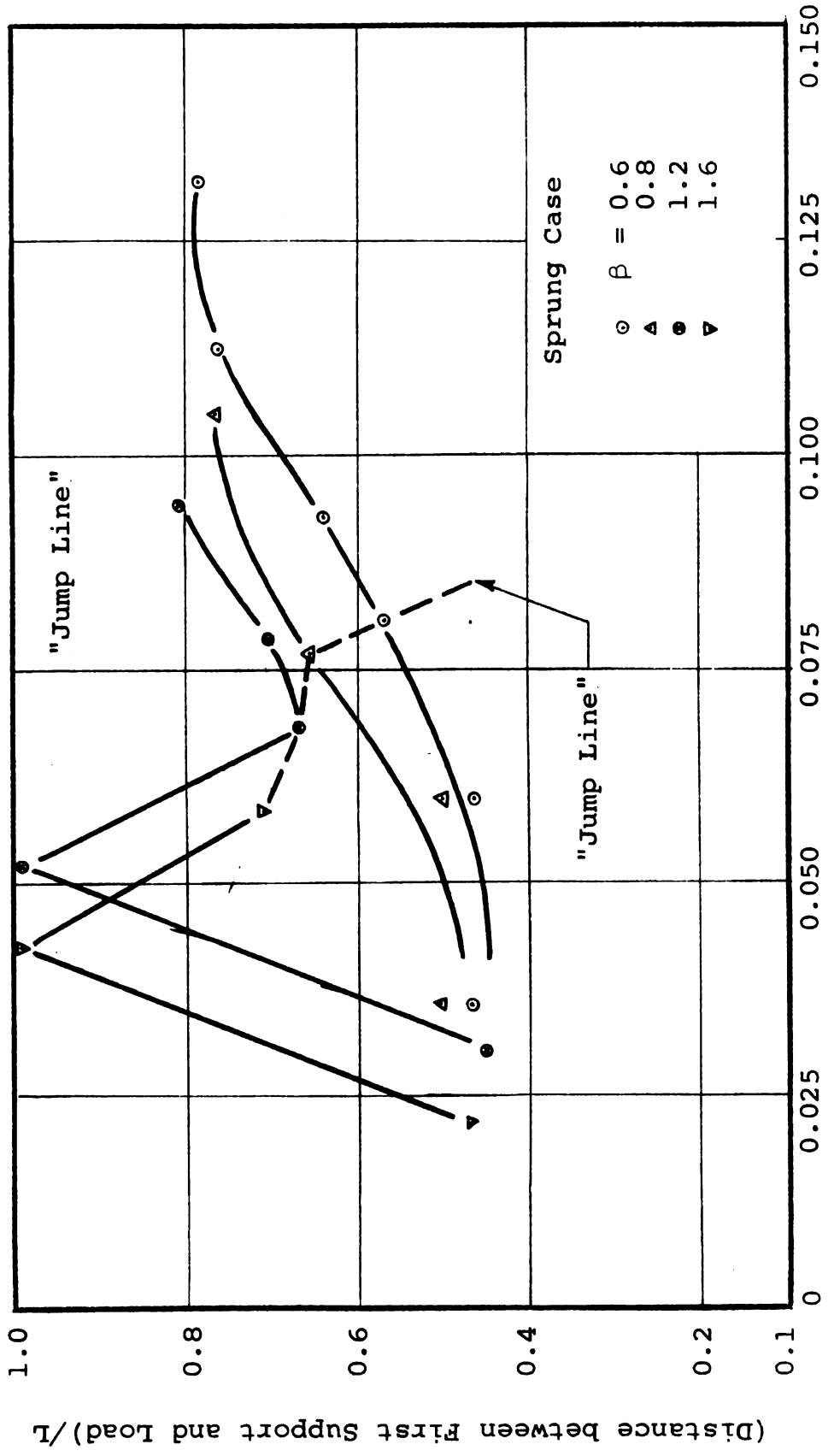

Figure 37--Location of maximum compressive spring force on first span.

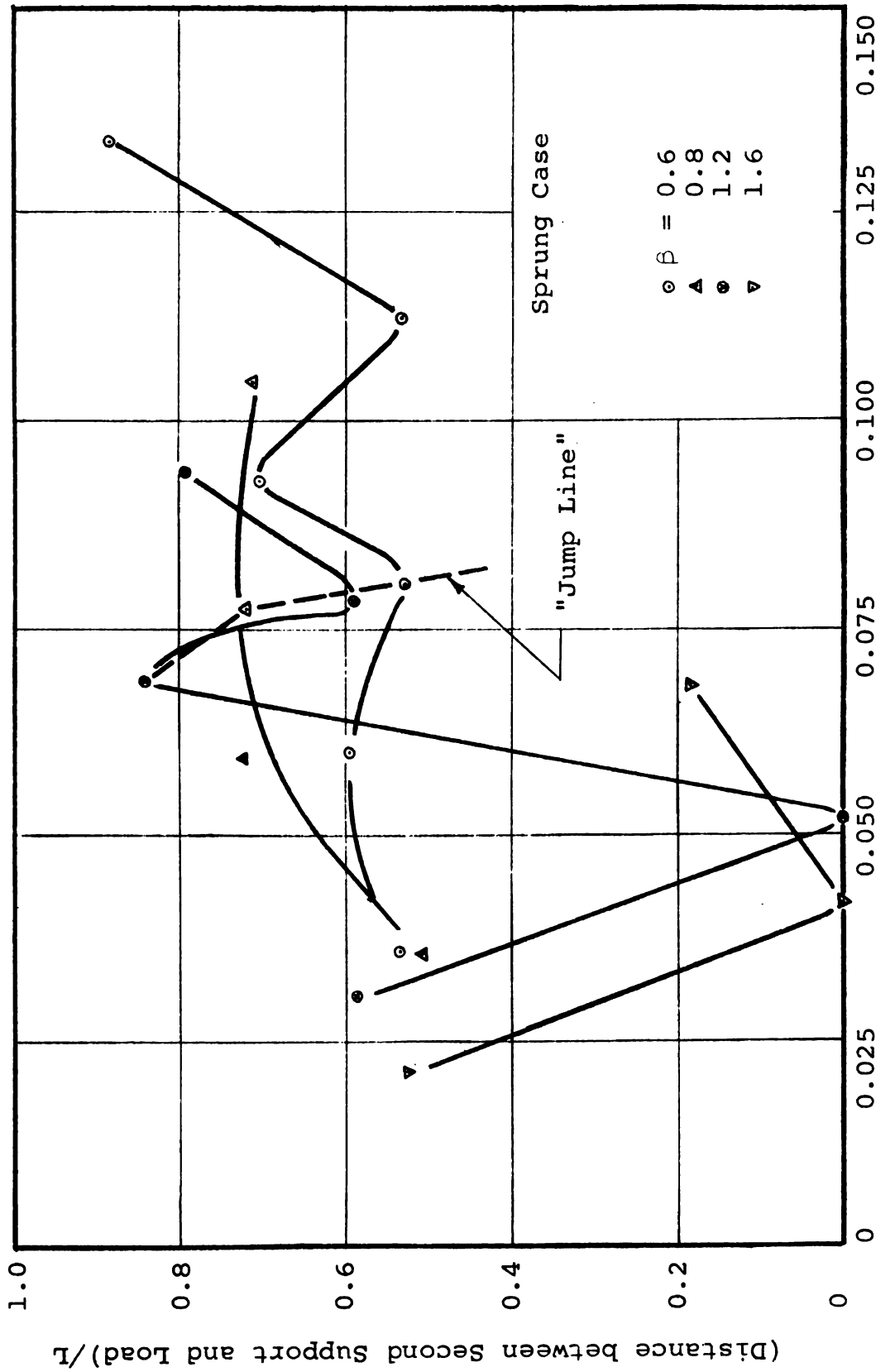

Figure 38--Location of maximum compressive spring force on second span.